Progress in Fractional Differentiation and Applications
*An International Journal*

http://dx.doi.org/10.18576/pfda/100313

# A review of fractional-order models for plant epidemiology

*Kottakkaran Sooppy Nisar*[1,*], *Muhammad Farman*[2,3], *Mahmoud Abdel-Aty* [4,5,6] *and Chokkalingam Ravichandran*[7]

[1]Department of Mathematics, College of Science and Humanities in Alkharj, Prince Sattam Bin Abdulaziz University, Alkharj 11942, Saudi Arabia
[2]Faculty of Arts and Sciences, Department of Mathematics, Near East University, Turkey
[3]Department of Computer Science and Mathematics, Lebanese American University, Beirut, Lebanon
[4]Deanship of Graduate Studies and Research, Ahlia University, P.O. Box 10878 Manama, Kingdom of Bahrain
[5]Jadara Research Center, Jadara University, Irbid, Jordan
[6]Mathematics Department, Faculty of Science, Sohag University, P.O. Box 82524, Sohag, Egypt
[7]Department of Mathematics, Kongunadu Arts and Science College (Autonomous), Coimbatore- 641 029, Tamil Nadu, India

Received: 25 Feb. 2024, Revised: 25 Mar. 2024, Accepted: 28 Mar. 2024
Published online: 1 Jul. 2024

**Abstract:** In the modern day, fractional operators are being utilized more and more to express problems and study the spread of epidemics, reflecting the growing interest in mathematical biology. Interventions pertaining to plant health and public health can benefit from the use of mathematical models to forecast the course of infectious illnesses, particularly those affecting plants. For the earth and all living beings, plants are extremely vital. Consequently, as it can offer valuable information on plant disease transmission, an understanding of plant disease dynamics is crucial. Among the most important maize diseases in the world are foliar diseases, which can be brought on by bacteria, viruses, or fungi. A mathematical model based on a hypothesis is expanded to include recovered plant species in order to observe the control effects of the early detection process. In the field, this strategy is now recognized as the conventional method. The importance of mathematical methods, especially fractional and integer calculus modeling, is emphasized by recent researchers when examining the dynamics of different disease models. Consequently, in order to monitor the continuous tracking of the disease's spread caused by the infection, the constructed model is transformed into a fractional order model using the fractal-fractional operator. An investigation, both qualitative and quantitative, is carried out to determine whether the newly constructed fractional order system is stable. The boundedness and uniqueness of the model are examined, as they are essential properties to understand the complex dynamics and guarantee robust conclusions. By applying Lipschitz conditions and linear growth, the global derivative is verified for true positivity and utilized to calculate the rate of disease effects based on each sub-compartment. Assessing the overall impact of the disease's spread and containment, the global stability of the system is examined through the application of Lyapunov's first derivative functions. The work finds the requirements for a solution to the suggested disease model and calculates reproductive numbers under particular conditions using a computationally effective approach to tackle both model and simulation difficulties. In the context of fractal-fractional operators, fractional refers to the fractional ordered derivative operator, and fractal refers to the spatial distribution of the disease. To view the actual dynamics of infection-induced virus transmission and control for maize foliar with different sizes and continuous monitoring, we use combine operators. We model both the symptomatic and asymptomatic consequences of maize foliar disease using MATLAB code, providing insights into the underlying dynamics of disease propagation and the possible suppressive effects of early detection. This paper presents an innovative approach that incorporates memory into the model by employing an equal-dimensional fractal-fractional operator. This approach takes into account the dynamic effects of illnesses on society and offers insightful information for analysis, choice-making, and illness prevention.

**Keywords:** Plant disease; Mathematical Model; Fractional Calculus; Stability Analysis.

## 1 Introduction

Biomathematics is a topic that blends biology and mathematics, with the goal of constructing mathematical representations to explain and address biological difficulties. In contrast, mathematical biology focuses on theoretical

* Corresponding author e-mail: n.sooppy@psau.edu.sa

experimentation [1]. Biomathematics is used in a variety of fields, including population genetics, epidemic modeling, and cellular neuroscience, to generate analytical and speculative models of biological and medical structures [2, 3]. An interdisciplinary topic called biomathematics, sometimes referred to as mathematical or theoretical biology, studies biological systems using computational and mathematical theory. Information is arranged, developing structures are examined, and biological systems and processes are frequently modeled using a variety of mathematical techniques and ideas [4, 5]. Numerous biological systems, such as the immune system, cancer cells, and the human genome, are studied in biomathematics. Even though biology has always used mathematics, modern research, especially in medicine, has relied more on computers, which has resulted in the development of new mathematical concepts [6]. To address major biological concerns in the 21st century, the next generation of scientists will require solid foundations in both biology and mathematics, together with great communication skills [7]. Epidemiological modeling has long been used in mathematical biology to analyze the spread of infectious diseases, but in recent years, its usage in disease management and control has increased dramatically. It is possible to solve biological model equations analytically or numerically to see how the system behaves at equilibrium or over time. In order to make decisions about epidemiological policies, several countries use mathematical models [8]. The study of mathematical epidemiology makes use of compartmental models to examine potential future epidemic scenarios and draw lessons from past outbreaks [9, 10].

These tools and technologies have proven invaluable in the development of effective disease prevention and control strategies. Pine wilt disease (PWD) is caused by the pinewood nematode *Bursaphelenchus xylophilus Nickle* and is dispersed by the Japanese pine sawyer beetle *Monochamus alternatus*. Japan was the first country to record PWD cases in 1905 [11]. After being discovered in Japan, PWD has spread to China, Taiwan, and Korea, seriously harming the pine forests of East Asia. Furthermore, in 1999, it was found in Portugal [12]. The country of Japan has suffered the most losses due to pine wilt disease. Throughout the 20th century, the disease expanded across extremely fragile Japanese red (P. densiflora) and Japanese black (P. thunbergiana) pine forests, wreaking havoc on both. In Iowa, Illinois, Missouri, Kentucky, eastern Kansas, and southeast Nebraska, scot pine has experienced considerable losses. PWD is now, by far, the greatest threat to forests around the globe [13]. Numerous kinds of pine trees can develop the dangerous and frequently fatal illness known as pine wilt, which is predominantly brought on by the pine wood worm. The quick wilting, browning of the needles, and final death of the tree are all caused by this minute roundworm, which obstructs water flow within the tree [14]. Early disease detection and management are crucial to halting the illness's spread to other trees. It is helpful to understand how a disease spreads and to identify the different components that contribute to the disease's spread through mathematical modeling. To analyze the disease's spread, various control strategies might be implemented for this goal. There aren't many developed mathematical models for pest management dynamics. Lee and Kim [15] and Shi and Song [16] investigated PWD transmission. The worldwide consistency of a host vector system for pine-wilt disease with nonlinear prevalence was ascertained by Lee and Lashari [17] in 2014. A fractional order epidemic model with a bilinear rate of incidence is empirically computed by Lia et al. [18] for the propagation of the pine wilt disease. Of course, here are more details about the pathogen causing pine wilt disease. The cause of the pine wilt disease is the microscopic roundworm referred to as the pine wood nematode (Bursaphelenchus xylophilus). The primary vectors that the worm uses to propagate are pine sawyer beetles (Monochamus spp.), which feed on affected trees before transferring the nematodes to trees that are healthy [19]. Affected Pine wilt disease primarily affects various species of pine trees, including Austrian pine (Pinus nigra), Scots pine (Pinus sylvestris), and Japanese black pine (Pinus thunbergii). Japanese black pine is particularly susceptible and often used as an indicator species for the disease [20]. Symptoms of infected trees typically exhibit rapid wilting, browning of needles, and overall decline within a matter of weeks. The needles may turn yellow or reddish-brown, starting from the tips and progressing downward. The tree's crown might show signs of dieback as well. Transmission of pine sawyer beetles spreading the nematode of pine wood from infected trees to healthy ones as they feed [21]. The nematode spreads within the tree's resin canals, blocking water transport and leading to wilting. The spread of pine wilt disease can occur both through natural beetle migration and the transportation of infested wood, such as lumber or wood chips [22].

Plant epidemiology is the study of illnesses that affect different plant families. It emphasizes how plants, without mobile defense and exhibiting characteristics unique to their species, rely on cellular inborn immunity to fight infections [23]. The promise of mathematical modeling is being highlighted by the growing use of these types of models to conduct studies by scientists studying vector-borne diseases, a plant virus epidemic, and trying to comprehend the patterns of transmission in host plants [24, 25]. Studying how infections spread and identifying the various factors that influence the transmission of diseases are made easier with the use of mathematical modeling. A discrete plant viral disease model with roguing and replanting that is derived from the continual example was studied by Luo et al. [26] using the popular backward Euler technique. The impact of a plant regeneration initiative's execution and the interplay between pathogen transmission and disease suppression are examined by Mark et al. [27] using sensitivity analyses of two substantially expressive simulation frameworks. These frameworks provide a summary of some efficient optimal controllers [28]. Mathematicians have employed a range of mathematical models to provide a foundation for specific illness modeling. In this order, [29] studies mathematically the behavior of the Jatropha curcas mosaic epidemic, which is carried out by whitefly vectors, by detecting oscillations in the model caused by a high infection rate.

Additionally, [30] frames the composition of a soil-borne plant epidemic in addition to host demographic information by demonstrating the essence of limit cycles.

The preventive and rehabilitative disinfectant model was developed in 2016 by Anggriani et al. [31]. It contains three parts for the plant population: susceptible, protected, and infectious. Their simulations showed that it is effective to use fungicides to lower population infection. In 2018, [32] developed a mathematical model of plant disease that included five elements: therapies that are protective and beneficial, as well as susceptible, exposed, infectious, post-infectious (removed), and protected. Investigators have used bilinear transfer of infections in their modeling investigations. Conversely, a nonlinear rate of incident is used in [33, 34] to characterize the development of vector-borne plant epidemics. Here, temporal delay among biological networks is incorporated to develop another modeling approach. Plant epidemic systems carried by delay vectors have the capacity to describe stability shifts, transcritical bifurcations, periodic fluctuations, and more. These observations are somewhat important in determining the degree of infection and illness control. A plant disease model presented in [35] was amended by Zhang et al. [36] by considering the length of plant incubation as an additional period to support the required modifications to the supplied dynamical pattern. Jackson [33] modified a model presented in [37] to account for the latent period in vectors and plant incubation cycles, therefore defining the processes of vector-borne epidemics in plants. A Caputo-type fractional mathematical model [38] was employed by researchers to examine the composition of a vector-borne plant epidemic. The goal of the research was to investigate the dynamics of the epidemic while accounting for memory effects, proving the value of fractional derivatives in plant epidemiology. Additionally, the research established the model's incorporation of memory through the use of Caputo derivatives with equal dimensionality. A fractional order model is used in a study [39] to provide a disease transmission model for a two-phase illness. Before becoming contagious, a susceptible person goes through an exposed period, and exposed plants can spread illness. The lack of knowledge regarding the general population's retention and acquisition processes for integer-order plant diseases is the cause of this increase. More precise and practical results were obtained by [40] when they used Caputo sense to study plant virus distribution driven by periodicity and rivalry between species, [41] yellow virus, in [42] curcas with farm consciousness and implementation delay. Using fractional and integer order differential equations, [43] provided models for the transmission that took into account both the vector and potato populations.

Plants are susceptible to infectious illnesses, which are mostly brought on by pathogens [44, 45]. In order to comprehend illness transmission, pinpoint the variables influencing disease spread, and enhance health management tactics, mathematical modeling has been thoroughly researched in this field. This vast body of research offers insightful information about the transmission of infectious illnesses in plants. The differential equations system used by the Plant Disease Transmission (PDT) model, which was initially presented in [46], splits plant and vector populations into three compartments. Differential equation systems are used in many studies to represent PDT, and models for positivity, boundedness, and local and global stability are analyzed. All EPs are assessed in these articles, and their local and global stability is covered [47, 48]. PDT for mosaic illness has recently been explained by the authors in [49] inside an FDE system. More specifically, research on the modeling of disease transmission in plants was looked at for several plant species. Food plants, such as rice [50], maize [51], [52], and plant diseases, such as Huanglongbing (HLB) disease in orange plants [53] and fractional order pine work in [54], are examples. The fractional order model (FOM), a novel mathematical framework for epidemic dynamics in plants, is presented in this study. The model governs fractional differential equations using Caputo derivatives; its accuracy in simulating actual-life situations to regulate the spread of epidemics has been enhanced by the modification of its parameters. The study also offers a thorough qualitative analysis, demonstrating the originality of the suggested solution by turning the issue into a fixed point problem and using Schauder's fixed-point theorem and the Banach contraction principle [55].

## 2 Fractional Calculus role in real life problems

The integral and differential operators of real or complex order are studied in the branch of mathematics known as fractional calculus [56]. i.e,

$$Dg(t) = \frac{d}{dt}g(t) \tag{1}$$

$$Jg(t) = \int_0^t g(u)du \tag{2}$$

The concept of fractional operators was first put forth with the development of integer ones. The first example of this can be found in a 1695 correspondence between Gottfried Wilhelm Leibniz and De L'Hopital, in which the question of semi-meaning derivatives is raised. Consequently, a number of well-known mathematicians developed an interest in this topic, including Letnikov, Laplace, Euler, Liouville, Riemann, Grunwald, and several others. The application of fractional

calculus theory has expanded rapidly since the 19th century and includes fractional differential equations (FDE), fractional geometry, and fractional dynamics, to name just a few. Fractional calculus has a plethora of applications nowadays [57,58]. It is reasonable to say that almost all branches of research and engineering make use of fractional calculus techniques and resources. For example, there are numerous advantageous applications in the domains of optical science, statistical and chemical physics, mechanical and electrical engineering, bioengineering, and other subjects [59]. Improvements in medicine, health care accessibility, and hygiene over the last 20 years have reduced the death and morbidity caused by viral infections. Nonetheless, the burden of infectious diseases remains high in low- and lower-middle-income nations, and there is still a strong correlation between mortality and morbidity and HIV infection, TB, malaria, and neglected tropical diseases. In the twenty-first century, illnesses have persisted in resurfacing and taking lives [60].

A mathematical model is a system in which our assumptions are explained and examined through the application of rules. Understanding the pathophysiology and mode of transmission is critical for the prevention and control of infectious illnesses. Using mathematical models based on interactions between hosts, infections, or vectors, scientists can predict rates of infection and the spread of disease [61]. A new mathematical model was developed by Khan et al. [62] in order to better understand the novel coronavirus. They gave a brief explanation of their mathematical results and the modeling of COVID-19 with the omicron version. Several studies have shown that fear's influence on people's behavior during an epidemic can reduce the number of new cases [63], [64]. The Ebola virus causes a dangerous and often fatal illness in humans. In west African countries, it is a highly contagious disease that has taken many lives. A mathematical model covering bat compartment, immune response recovery, and vaccine was developed in [65] to study the population dynamics of Ebola virus infections. [66] looked at a deterministic mathematical model to assess successful interventions for meningitis and pneumonia co-infection and to offer sane guidance to the general public, policy or decision makers, and program implementers. A wealth of resources is at your disposal for measles modeling. Math has emerged as a helpful tool for comprehending the molecular mechanism behind the measles spread [67]. It can also be used to suggest the safest path to measles eradication, including when vaccination should be administered [68]. Sowole et al. [69] developed a mathematical deterministic modeling approach using Nigerian-specific data to anticipate the measles disease. A control measure was introduced into the susceptible and subjected classes in order to investigate the prevalence and management of measles. Liu et al. [70] looked at stochastic control systems and optimal control theories to control the virus's propagation utilizing environmental factors. Peter et al. [71] examined the impact of particular prophylactic strategies for effective measles control. Because of its non-local characteristics, fractional calculus is a branch of mathematics that studies real and complex number powers of differentiation and integration operators. It allows for derivatives and integrals of any non-negative order and is utilized in historical modeling [72]. It is currently used in many different medical specialties and is a useful tool for adding memory and genetic components to systems [73]. A fractional derivative can have any arbitrary order as its foundation, real or complex. Gottfried Wilhelm Leibniz first mentioned them in a 1695 letter to Guillaume de l'Hôpital [74]. One of Niels Henrik Abel's early publications contains every element of fractional calculus. Therefore, at the time his article was published, Niels Henrik Abel was the originator of the entire fractional-order calculus situation [75]. The differentiating formula for the exponential function was employed by Liouville in his 1832 formulation of fractional calculus. The issue was covered in Riemann's most important article, ten years after his passing. Many writers have made contributions [76] and fractional models are frequently employed in [77]. The most frequently used operators connect a local derivative with a function that has different kernels [78], [79], stability theory in [80]. On the other hand, a lot of real-world phenomena-like volatility, waterways, permeable media, medicine, and Darcy's law-show complicated fractal behavior. Atangana provided FF operators, which are necessary for the kernel to include operators engaging nonlocal differentiation in this scenario [81].

Fractional calculus is being used in an increasing number of disciplines to comprehend intricate dynamical systems with reminiscence consequences. The q-homotopy analysis transform was utilized by [82] for resolving the fractional order mathematical model of a fatal illness in pregnant women computationally. [83] investigated the behavior of a piecewise Covid-19 mathematical framework with a quarantine class and vaccination using an epidemic model. They examined fractional, unpredictable, and consistent forms for different stages. In [84] used non-singular and non-local kernels to develop a mathematical model for tuberculosis cases in KPK, Pakistan, from 2002 to 2017. In [85] used a recently proposed numerical method to approximate the fractional ABC derivative and developed a fractional order model for Hepatitis-B infection by means of the ABC derivative and some applications in [86, 87]. Some researchers in [88] created a listeriosis model by utilizing derivatives of the FF order in the meanings of Caputo, Atangana-Baleanu, and others. beneficial and productive study through fractional order is designed in [89–92]. In [93] illustrates the possible outcomes of getting into contact with a deceased person who is communicable in order to disseminate this illness. They also created this epidemic model using the fractional Adams-Bashforth-Moulton numerical approach. Treatment and stem cells in a fractional-order cancer system to study the effects of infection on humans. To investigate the idea, the Sumudu transform and an extremely effective numerical method were applied [94, 95]. The challenge was solved by using a crude model that linearizes the four FODEs at each time step. A measles epidemiological model was fractionalized by [96] employing a non-local operator of the Caputo type, and the results were compared with the

classical version. They found that fractional counterparts outperform classical counterparts regardless of whether the real data set is expanding or contracting. An analytical solution to the measles transmission model with three vaccination doses was provided by [97] via the CF fractional derivative. The proposed solution was based on the Adomian decomposition approach and the Laplace transform [98]. Using ABC fractional-order derivative, the study [99] generalizes a plant-nectar-pollinator (PNP) model and shows higher performance under fractional derivative, indicating an improved comprehension of PNP behavior with non-local impacts. The piecewise plant-pathogen-herbivore interactions model was updated in the study [100], and it was verified by numerical simulations in fractional and piecewise fractional representations. A semi-analytical resolution for the Pine Wilt disease model was proposed by researchers [101], who combined the Adomian decomposition method with the Caputo-Fabrizio fractional derivative and Laplace transform. In order to comprehend the primary challenges caused by the yellow virus in the production of Capsicum annuum, researchers [102] have examined the fractional-order model of chili plants via an ABC derivative. A model for yellow virus proliferation in red chili plants was created by researchers [103], who used mathematical simulations and a fractional derivative framework to analyze important components. Numerous writers have conducted extensive research and works to examine the dynamics of infectious diseases in fractional order models [104]- [119]. We go over the following basic definitions, which are necessary to comprehend our proposed system.

## 3 Fundamental Definitions

With $\mathsf{P} \subset \mathsf{J}$, let $\mathsf{J}^n$ be Euclidean space, and let $\mathsf{P}$ be a specific interval along the real line. We assume that for some $t \in \mathsf{P}$, $\mathsf{P} = [t_0, \mathsf{T}]$. This allows us to show that $\bar{\mathsf{P}} = (t_0, \mathsf{T})$. Assume that there is clear continuity in the function $M : \mathsf{P} \to \mathsf{J}$.

**Definition 1.** [120] The definition of the Riemann-Liouville fractional derivative for $n-1 < \alpha \leq n$, $n \in \mathsf{N}$, is

$$ {}^{RL}_{t_0}\mathrm{D}^{\alpha}_{t} h(t) = \frac{1}{\Gamma(n-\alpha)} \Big(\frac{d}{dt}\Big)^n \int_{t_0}^{t} (t-\rho)^{n-\alpha-1} h(\rho) d\rho, \;\; -\infty \leq t_0 < t \leq \infty \;\; , t \in \bar{\mathsf{P}}. \tag{3} $$

**Definition 2.** [120] The Riemann-Liouville fractional integral for $\alpha > 0$ is defined as

$$ {}^{RL}_{t_0}\mathrm{I}^{\alpha}_{t} h(t) = \frac{1}{\Gamma(\alpha)} \int_{t_0}^{t} h(\rho)(t-\rho)^{\alpha-1} d\rho, \;\; -\infty \leq t_0 < t \leq \infty \;\; , t \in \bar{\mathsf{P}}. \tag{4} $$

**Definition 3.** [120] The Caputo fractional derivative is defined by

$$ {}^{RL}_{t_0}\mathrm{D}^{\alpha}_{t} h(t) = \frac{1}{\Gamma(n-\alpha)} \int_{t_0}^{t} \frac{\big(\frac{d}{dt}\big)^n h(\rho)}{(t-\rho)^{\alpha+1-n}} d\rho, \;\; -\infty \leq t_0 < t \leq \infty \;\; , t \in \bar{\mathsf{P}}. \tag{5} $$

At initial point $t = 0$, we have

$$ {}^{C}_{0}\mathrm{D}^{\alpha}_{t} h(t) = \frac{1}{\Gamma(1-\alpha)} \int_{0}^{t} h'(\vartheta)(t-\rho)^{-\alpha} d\rho / \tag{6} $$

*Remark.It is clear from the definitions that*

$$ {}^{C}_{0}\mathrm{D}^{\alpha}_{t} h(t) = {}^{RL}_{a}I^{1-\alpha}_{t} h'(t) \tag{7} $$

**Definition 4.** [121] About $\alpha \in [0,1]$ then allow the following functions to exist: $Z_0, Z_1 : [0,1] \times \mathsf{R} \to [0,\infty)$ be continuous in order for $\forall t \in \mathsf{R}$, then we can define the Conformable derivative by

$$ {}^{P}\mathrm{D}^{\alpha}_{t} h(t) = Z_1(\alpha,t)h(t) + Z_0(\alpha,t)h'(t). \tag{8} $$

Here, we specify

$$ Z_0(\alpha,t) = \alpha t^{1-\alpha} \;, \; Z_1(\alpha,t) = (1-\alpha)t^{\alpha}. \tag{9} $$

When $Z_0$ and $Z_1$ are constant with regard to $t$, as in a particular instance of proportional derivatives, the Constant Proportional (CP) derivative is defined by

$$ {}^{CP}\mathrm{D}^{\alpha}_{t} h(t) = Z_1(\alpha)h(t) + Z_0(\alpha)h'(t). \tag{10} $$

**Definition 5.**The hybrid fractional derivative in [122] is defines as

$$\begin{aligned}{}_0^{PC}\mathrm{D}_t^{\alpha}h(t) &= \frac{1}{\Gamma(1-\alpha)}\int_0^t \left\{Z_1(\alpha,\rho)h(\rho)+Z_0(\alpha,\rho)h'(\rho)\right\}(t-\rho)^{-\alpha}d\rho \\ &= {}_0^{RL}I_t^{1-\alpha}\left[Z_1(\alpha,t)h(t)+Z_0(\alpha,t)h'(t)\right]. \end{aligned} \tag{11}$$

As a particular instance of PC, the Constant Proportional-Caputo (CPC) derivative is expressed as follows:

$$\begin{aligned}{}_0^{CPC}\mathrm{D}_t^{\alpha}h(t) &= \frac{1}{\Gamma(1-\alpha)}\int_0^t \left\{Z_1(\alpha)h(\rho)+Z_0(\alpha)h'(\rho)\right\}(t-\rho)^{-\alpha}d\rho \\ &= Z_1(\alpha)\,{}_0^{RL}I_t^{1-\alpha}h(t)+Z_0(\alpha)\,{}_0^{C}D_t^{\alpha}h(t). \end{aligned} \tag{12}$$

*Remark. [122] If $\alpha = 0$, then*

$$\lim_{\alpha\to 0}{}_0^{PC}\mathrm{D}_t^{\alpha}h(t) = \lim_{\alpha\to 0}{}_0^{CPC}\mathrm{D}_t^{\alpha}h(t) = \int_0^t h(\rho)d\rho. \tag{13}$$

*and, if $\alpha = 1$, we get*

$$\lim_{\alpha\to 1}{}_0^{PC}\mathrm{D}_t^{\alpha}h(t) = \lim_{\alpha\to 1}{}_0^{CPC}\mathrm{D}_t^{\alpha}h(t) = h'(\rho). \tag{14}$$

**Definition 6.** [122] The inverse operator of the CPC derivative is as follows:

$$\begin{aligned}{}_0^{CPC}\mathrm{D}_t^{\alpha}h(t) &= \frac{1}{Z_0(\alpha)}\int_0^t (t-\rho)^{\alpha-1}E_{1,\alpha}\left(-\frac{Z_1(\alpha)}{Z_0(\alpha)}(t-\rho)\right)h(\rho)d\rho \\ &= \sum_{n=0}^{\infty}\frac{(-Z_1(\alpha))^n}{(Z_0(\alpha))^{n+1}}\,{}_0^{RL}\mathrm{I}_t^{\alpha+n}h(t). \end{aligned} \tag{15}$$

which satisfies

$${}_0^{CPC}\mathrm{D}_t^{\alpha}\left[{}_0^{CPC}\mathrm{I}_t^{\alpha}h(t)\right] = h(t) - \frac{t^{-\alpha}}{\Gamma(1-\alpha)}\lim_{t\to 0}{}_0^{RL}\mathrm{I}_t^{n}h(t); \tag{16}$$

$${}_0^{CPC}\mathrm{I}_t^{\alpha}\left[{}_0^{CPC}\mathrm{D}_t^{\alpha}h(t)\right] = h(t) - h(0)\exp\left[\frac{-Z_1(\alpha)}{Z_0(\alpha)}t\right]. \tag{17}$$

**Theorem 1.**The Laplace transform for the CPC operator looks like this:

$$\mathscr{L}({}^{CPC}\mathrm{D}_t^{\alpha}h(t)) = \left(\frac{Z_1(\alpha)}{\mathfrak{S}}+Z_0(\alpha)\right)\mathfrak{S}^{\alpha}\widetilde{h}(\mathfrak{S}) - Z_0\mathfrak{S}^{\alpha-1}h(0), \tag{18}$$

*Proof.*Remember the Caputo derivative and the RL integral's Laplace transforms. For $0 < \alpha < 1$,

$$\mathscr{L}\left({}^{RL}\mathrm{I}_t^{\alpha}h(t)\right) = \mathfrak{S}^{-\alpha}\widetilde{h}(S), \tag{19}$$

$$\mathscr{L}\left({}^{C}\mathrm{D}_t^{\alpha}h(t)\right) = \mathfrak{S}^{\alpha}\widetilde{h}(S) - \mathfrak{S}^{\alpha-1}h(0). \tag{20}$$

Hence,

$$\begin{aligned}\mathscr{L}\left({}^{CPC}\mathrm{D}_t^{\alpha}h(t)\right) &= \mathscr{L}\left(Z_1(\alpha)\,{}^{RL}\mathrm{I}_t^{1-\alpha}h(t)+Z_0(\alpha)\,{}^{C}\mathrm{D}_t^{\alpha}h(t)\right) \\ &= Z_1(\alpha)\mathscr{L}\left({}^{RL}\mathrm{I}_t^{1-\alpha}h(t)\right)+Z_0(\alpha)\mathscr{L}\left({}^{C}\mathrm{D}_t^{\alpha}h(t)\right) \\ &= Z_1(\alpha)\mathfrak{S}^{1-\alpha}\widetilde{h}(\mathfrak{S})+Z_0(\alpha)\left[\mathfrak{S}^{\alpha}\widetilde{h}(\mathfrak{S})-\mathfrak{S}^{\alpha-1}h(0)\right] \\ &= \left[Z_1(\alpha)\mathfrak{S}^{\alpha-1}+Z_0\mathfrak{S}^{\alpha}\right]\widetilde{h}(\mathfrak{S}) - Z_0(\alpha)\mathfrak{S}^{\alpha-1}h(0). \end{aligned} \tag{21}$$

**Definition 7.** [123] If $j \in \mathsf{C}$ and $\alpha \in (0,1)$, then $Re(j) > 0$. The function $h$ has a left generalized proportional derivative of order $\alpha$, which may be found using

$${}_u\mathrm{D}_t^{j,\alpha}h(t) = \frac{\mathrm{D}^{n,\alpha}}{\alpha^{n-j}\Gamma(n-j)}\int_u^t e^{\frac{\alpha-1}{\alpha}(t-\rho)}(t-\rho)^{n-j-1}h(\rho)d\rho. \tag{22}$$

$n = \lfloor j \rfloor + 1$.

*Remark. [123] Assume that* $j,q \in \mathsf{C}$ *and* $Re(q) > 0$, $Re(j) \geq 0$. *Then for* $0 < \alpha \leq 1$, *we find*

$$\left\{ \mathrm{I}_u^{j,\alpha} e^{\frac{\alpha-1}{\alpha}(t)} (t-y)^{q-1} \right\}(t) = \frac{\Gamma(q)}{\alpha^j \Gamma(j+q)} e^{\frac{\alpha-1}{\alpha}(t)} (t-y)^{j+q-1}, \tag{23}$$

$$\left\{ \mathrm{I}_v^{j,\alpha} e^{\frac{\alpha-1}{\alpha}(z-t)} (z-t)^{q-1} \right\}(t) = \frac{\Gamma(q)}{\alpha^j \Gamma(j+q)} e^{\frac{\alpha-1}{\alpha}(z-t)} (z-t)^{j+q-1}. \tag{24}$$

**Definition 8.** [123] Let $j \in (n-1,n)$, $n \in \mathsf{N}$, $\alpha \in (0,1)$ and $w \in [0,1]$. The left/right Hilfer generalized proportional derivative of a function $h$ of order j and class w is given by

$$\mathrm{D}_u^{j,w,\alpha} h(t) = \mathrm{I}_u^{w(n-j),\alpha} \left\{ \mathrm{D}^{\alpha} \left( \mathrm{I}_u^{(1-w)(n-j),\alpha} h(t) \right) \right\}. \tag{25}$$

Where

$$\mathrm{D}^{\alpha} h(t) = (1-\alpha) h(t) + \alpha h'(t), \tag{26}$$

At $n = 1$, the equation (25) simplifies to

$$\mathrm{D}_u^{j,w,\alpha} h(t) = \mathrm{I}_u^{w(1-j),\alpha} \left\{ \mathrm{D}^{\alpha} \left( \mathrm{I}_u^{(1-w)(1-j),\alpha} h(t) \right) \right\}. \tag{27}$$

## 4 Description of Fractional order plant epidemiological models

Two fractional dynamic mathematical models for a mosaic plant epidemic brought on by begomoviruses and whiteflies were created by Pushpendra et al. [124]. In order to enhance the growth of plants and guard against infection, they took into consideration natural microbial biostimulants. The structure of the model was defined by the study utilizing Caputo and Atangana-Baleanu fractional derivatives, and existence and uniqueness studies were carried out via fixed point theory and the Picard-Lindelof method. The study emphasizes the significance of determining the disease's main optimum control methods. A semi-analytical resolution to the Pine Wilt disease model was proposed by Kamal et al. [125], who used the Caputo-Fabrizio fractional derivative. When attempting to solve nonlinear differential equations of fractional order, they combined the Laplace transform with the Adomian decomposition approach, which is a very effective tool. The solution and assessment are validated by the results. The maize streak virus, which affects more than 80 different species of grass in addition to maize, was investigated by Joseph et al. [126]. The main vectors on maize fields are leafhoppers, and Holling's Type III functional response is used to study the relationship between them in a Caputo fractal-fractional derivative approach. The model was numerically simulated by the study using the Newton polynomial scheme, and it identified unique positive solutions within a viable domain. The association between state characteristics and epidemiological factors was also investigated in this study. In their study of the availability of food in the context of population growth, Pawan et al. [127] concentrated on staple plant-based diets and agriculture. They employed Caputo fractional derivative and Caputo–Fabrizio fractional derivative operators of arbitrary order in a fractional order model to investigate the behavior of two-stage plant diseases. The usefulness of replanting in "inter-row" to reduce replant disease in apple orchards was investigated by Markus et al. [128], with an emphasis on the interaction between plants and microorganisms.

The work of Massimo et al. [129] is centered on the selection of innovative biological control agents (BCAs) to combat plant pathogens that are carried by the soil. Large-scale implementation requires quick screening techniques, and digital technology can be applied for quick performance evaluations and early illness identification. In order to improve understanding about crop management and address the decline in apple orchard land in Central Europe, Manici et al. [130] performed a transnational survey on apple root-associated bacteria. Farman et al. [131] created a sustainable method using fractal fractional derivatives to examine the dynamics of plant infection. Studies that were both qualitative and quantitative were carried out to confirm the presence and uniqueness of the model. The positiveness and boundedness of the solutions were confirmed using linear growth and Lipschitz criteria. We also evaluated both local and global stability with the Lyapunov function. The fractional order model for plant diseases was first presented by El-sayed et al. [132] in a two-stage infection, highlighting the significance of comprehending plant disease dynamics for comprehension of transmission and mitigation of plant-related problems. Tariq et al. [133] investigated how growing global population affects food requirements, specifically with regard to plant diseases. Utilizing Atangana-Baleanu derivatives in the sense of Caputo, they employed mathematical models to investigate the dynamics of plant disease treatments (ABC). They investigated the existence and distinctiveness of treatments for fractional models of plant disease prevention and cure, employing Lagrange interpolation for numerical simulations and particular parameters. Ali et al. [134] have used Caputo derivatives to create a new mathematical model for the evolution of epidemics in plants. The parameters have been adjusted to align both dimensions, improving the precision of the model in simulating actual situations involving the containment of disease spread. The paper contains a thorough qualitative analysis that demonstrates the originality of the suggested

solution by turning the issue into a fixed point problem and using Schauder's fixed-point hypothesis and the Banach contraction theorem. Sunil et al. [135] used Caputo's operator to analyze field data in order to construct a computational framework for the tritrophic food chain population. The model explores the prospect of getting fresh chaotic patterns using a singular fractional operator that is composed of a host, a pest, and a predator. The study also looks at how climate change is affecting the world's food supply, including the staple crop potato. The research emphasizes how important it is to comprehend and manage this intricate ecology more effectively. A potato disease model in a fractional-order derivative that includes a nonlocal and nonsingular operator (AB) is presented in the research [136]. The Banach space technique is utilized for determining the existence and uniqueness of solutions, as well as the reproduction number and steady phases. To ascertain stability, Hyers-Ulam stability is also looked at. Jeger and colleagues [137] investigated plant viruses, which are generally spread by arthropods, especially insects that are part of the hoop family. They classified plant-virus illnesses into four groups according to how the viruses interacted with the vector and how they spread. Persistent viruses are ingested, penetrate the gut wall, and may go to the salivary glands. Nonpersistent viruses are typically located in the insect's stylet. Behre examined the effects of protective netting, roguing, and insecticide spraying as control measures for the tomato yellow leaf curl virus. It develops and examines a deterministic framework for the dynamics of disease transfer, taking into account the fundamental reproduction number, the occurrence and stability of endemic and disease-free equilibria, and a stable control scenario. The research is predicated on a [138].

## *4.1 Power Law Kernel*

We obtained some important and useful results from contemporary calculus and nonlinear dynamics.

**Definition 9.***Assume that $h(t)$ is a function that is not necessarily differentiable. Given $\beta$ as the fractal dimension and $\alpha$ as the fractional order, let $0 < \alpha \leq 1$ and $0 < \beta \leq 1$. [139] defines a fractal fractional derivative with power law kernel as follows:*

$$^{FFP}D_{0,t}^{\alpha,\beta}h(t) = \frac{1}{\Gamma(1-\alpha)}\frac{d}{dt^{\beta}}\int_0^t h(\rho)(t-\rho)^{-\alpha}d\rho, \tag{28}$$

*where*

$$\frac{dh(t)}{dt^{\beta}} = \lim_{t\to t_1}(2-\beta)\frac{h(t)-h(t_1)}{t^{2-\beta}-t_1^{2-\beta}}. \tag{29}$$

*The corresponding fractional integral is*

$$^{FFP}I_{0,t}^{\alpha,\beta}h(t) = \frac{1}{\Gamma(\alpha)}\int_0^t (t-\rho)^{\alpha-1}\rho^{1-\beta}h(\rho)d\rho. \tag{30}$$

### 4.1.1 Application I (Vector Borne Plant Disease)

The study of the detrimental impact of viruses or deadly diseases on plants is known as plant epidemiology. The model's characteristics are examined in this work, including its genesis, nonnegativity, boundedness of solutions, equilibrium point stability, and disease-free and endemic conditions [140]. With the Caputo fractional derivative obtained from the singular-type kernel, many mathematicians have suggested nonclassical type derivatives since the beginning of the decade. This study generalizes a Caputo-type model with equal dimension time on both sides by reformulating an integer-order model into the Caputo sense.

$$\begin{cases} {}^{C}D_t^{\lambda}Q(t) = g^{\lambda}Q\left\{1-\frac{Q+R}{k^{\lambda}}\right\} - \frac{\Omega^{\lambda}QS}{1+\delta^{\lambda}Q+b^{\lambda}S}, \\ {}^{C}D_t^{\lambda}R(t) = \frac{\Omega^{\lambda}e^{-\beta^{\lambda}\tau}Q(t-\tau)S(t-\tau)}{1+\delta^{\lambda}Q(t-\tau)+b^{\lambda}S(t-\tau)} - \left(\beta^{\lambda}+\Lambda^{\lambda}\right)R, \\ {}^{C}D_t^{\lambda}S(t) = \alpha^{\lambda}R - \gamma^{\lambda}S. \end{cases} \tag{31}$$

The main goal of this replacement is to imitate memory effects by studying the dynamics of an integer-order model at fractional-order values.

### 4.1.2 Application II (Mosaic Plant Disease)

The fractional-order mathematical model of mosaic illness, first presented in [141], is examined here. The entire population is divided into four major classes, including the plant and vector populations. There are two classes in the

plant (host) class: healthy or uninfected plants $P_s$ and infected plants $P_i$. There are two classifications in the vector population: susceptible or uninfected $V_s$ and infected $V_i$. Hence, the model for mosaic illness is provided by

$$\begin{cases} {}^{C}D_t^{\lambda} P_s(t) = g(b)P_s\left\{1-\frac{P_s-P_i}{k}\right\} - \eta(b)V_iP_s, \\ {}^{C}D_t^{\lambda} P_i(t) = \eta(b)V_iP_s - \beta P_i, \\ {}^{C}D_t^{\lambda} V_s(t) = \Lambda(V_i+V_s)\left\{1-\frac{V_s-V_i}{\alpha(P_s+P_i)}\right\} - \gamma V_sP_i - d(b)(P_s+P_i)V_s, \\ {}^{C}D_t^{\lambda} V_i(t) = \gamma V_sP_i - \delta V_i - d(b)(P_s+P_i)V_i. \end{cases} \tag{32}$$

This study uses Caputo fractional derivatives to propose an optimal control problem for the mosaic disease model. Microbial biostimulants (MBs) derived from natural sources are employed to enhance plant growth and provide defense against mosaic infection. To find out more about how spraying and roguing, two more ideal controls, affect mosaic spread, they are used. The forward-backward sweep method is used to execute experiments at different fractional order levels. According to the study, the only control that can successfully halt the spread of mosaics in the presence of MBs is roguing.

#### 4.1.3 Application III

By applying a generalized Liouville Caputo type fractional operator, a fractional-order model is substituted for the classical one. The objective is to perform dynamical changes simulations at different fractional-order levels. Whether a solution exists and if they are appropriate for the particular model depends on the usage of non-integer order derivatives. In research on ecology, fractional derivatives work well. The model's fractional sense generalization is derived in [142] in order to satisfy this criterion.

$$\begin{cases} {}^{C}D_t^{\phi,\rho} C(t) = \frac{PU}{C+1} - \frac{\alpha UC}{C+v_2} - \frac{\eta CV}{C+v_3} - C, \\ {}^{C}D_t^{\phi,\rho} U(t) = \left\{\frac{QC}{C+v_1} - U\right\}U - \frac{UV}{U+\kappa} - \gamma U, \\ {}^{C}D_t^{\phi,\rho} V(t) = \frac{\omega C^2}{C^2+v_4^2}\frac{UV}{U+\kappa} - \beta V. \end{cases} \tag{33}$$

This research focuses on studying the dynamics of a coupled plankton-oxygen model using three non-linear differential equations. Ocean dynamics significantly impact global climate change and environmental creation.

#### 4.1.4 Application IV (Plant Virus Model)

A fractional operator of the extended Riemann Liouville Caputo type is used to replace the traditional framework with a fractional-order model. Simulating dynamical changes at different fractional-order levels is the aim. To make sure that they are appropriate for the particular model and to determine whether a solution exists, non-integer order derivatives must be used. Ecological research can benefit from the use of fractional derivatives. [143] derives the model's fractional sense generalization in order to satisfy this criterion.

$$\begin{cases} {}^{C}D_t^{\phi} S(t) = \mu(\kappa - S) + d_I - \frac{\beta Y}{1+\alpha Y}S, \\ {}^{C}D_t^{\phi} I(t) = \frac{\beta Y}{1+\alpha Y}S - (d+\mu+\gamma)I, \\ {}^{C}D_t^{\phi} X(t) = \Lambda - \frac{\beta_1 I}{1+\alpha_1 I}X - \frac{c_1 X}{1+\alpha_3 X}P - mX, \\ {}^{C}D_t^{\phi} Y(t) = \frac{\beta_1 I}{1+\alpha_1 I}X - \frac{c_2 Y}{1+\alpha_3 Y}P - mY, \\ {}^{C}D_t^{\phi} P(t) = \Lambda_P + \frac{\alpha_4 c_1 X}{1+\alpha_3 X}P + \frac{\alpha_4 c_2 Y}{1+\alpha_3 Y}P - \delta P. \end{cases} \tag{34}$$

This study presents an application for reproduction number for epidemic models utilizing the next generation matrix approach, and explores the characteristics of the plant virus model using its fractional order equivalent. Additionally, the study proves that there are solutions to this fractional order system and that they are unique. Additionally, the authors include figures derived from the numerical method.

### *4.2 Exponential Decay Kernel*

**Definition 10.***Assume that $h(t)$ is a function that is not necessarily differentiable. Given $\beta$ as the fractal dimension and $\alpha$ as the fractional order, let $0 < \alpha \leq 1$ and $0 < \beta \leq 1$. [139] defines a fractal fractional derivative with exponential decay*

*kernel as follows:*

$$^{FFE}D_{0,t}^{\alpha,\beta}h(t)=\frac{M(\alpha)}{1-\alpha}\frac{d}{dt^{\beta}}\int_0^t h(\rho)exp\left[-\frac{\alpha}{1-\alpha}(t-\rho)\right]d\rho. \tag{35}$$

*The associated integral is given by*

$$^{FFE}J_{0,t}^{\alpha,\beta}h(t)=\frac{1-\alpha}{M(\alpha)}t^{1-\beta}h(t)+\frac{\alpha}{M(\alpha)}\int_0^t \rho^{1-\beta}h(\rho)d\rho. \tag{36}$$

#### 4.2.1 Application I (yellow virus in red chili plants)

We present a compartmental model for the dynamics of the Yellow virus in red chili plants, focusing on the origins and recurrence of hypothesized epidemics. The model, proposed by Sajjad et al. [144], is represented by a set of nonlinear system of differential equations, providing a comprehensive understanding of the virus's dynamics.

$$\begin{cases} ^{\mathscr{CF}}\mathbb{D}_t^{\vartheta}S_v(t)=A-\alpha S_v-\beta_1(1-\delta_P)S_vI_{BT}-\mu_PS_v,\\ ^{\mathscr{CF}}\mathbb{D}_t^{\vartheta}I_v(t)=-\beta_1(1-\delta_P)S_vI_{BT}-\mu_PI_v,\\ ^{\mathscr{CF}}\mathbb{D}_t^{\vartheta}S_g(t)=\alpha S_v-\beta_2(1-\delta_P)S_gI_{BT}-\mu_PS_g,\\ ^{\mathscr{CF}}\mathbb{D}_t^{\vartheta}I_g(t)=\beta_2(1-\delta_P)S_gI_{BT}-\mu_PI_g,\\ ^{\mathscr{CF}}\mathbb{D}_t^{\vartheta}S_{BT}(t)=rS_{BT}\left(1-\frac{S_{BT}}{K}\right)-\gamma_1(1-\delta_P)I_vS_{BT}-\gamma_2(1-\delta_P)I_gS_{BT}-\theta_1\delta_PS_{BT}N_P-\mu_1S_{BT},\\ ^{\mathscr{CF}}\mathbb{D}_t^{\vartheta}I_{BT}(t)=\gamma_1(1-\delta_P)I_vS_{BT}+\gamma_2(1-\delta_P)I_gS_{BT}-\theta_1\delta_PI_{BT}N_P-\mu_1I_{BT}. \end{cases} \tag{37}$$

This work employs the Caputo-Fabrizio operator in fixed point theory to determine the existence, uniqueness, and stability criteria for the fractional order yellow virus in the red chilli model. The Laplace transform method is combined with a dependable iterative method in the iterative Laplace transform approach, and the fractional derivative methodology is new for biological models. Charts are used to illustrate numerical simulations based on the analysis of parameters that describe the evolution of illness.

### *4.3 Mittag-Leffler Kernel*

**Definition 11.***Assume that $h(t)$ is a function that is not necessarily differentiable. Given $\beta$ as the fractal dimension and $\alpha$ as the fractional order, let $0<\alpha\leq 1$ and $0<\beta\leq 1$. [139] defines a fractal fractional derivative with Mittag Leffler kernel as follows:*

$$^{FFM}D_{0,t}^{\alpha,\beta}f(t)=\frac{AB(\alpha)}{1-\alpha}\frac{d}{dt^{\beta}}\int_0^t f(\delta)E_{\alpha}\left[-\frac{\alpha}{1-\alpha}(t-\delta)^{\alpha}\right]d\delta, \tag{38}$$

*The associated integral is given by*

$$^{FFM}J_{0,t}^{\alpha,\beta}f(t)=\frac{1-\alpha}{AB(\alpha)}t^{1-\beta}f(t)+\frac{\alpha}{AB(\alpha)\Gamma(\alpha)}\int_0^t \delta^{1-\beta}(t-\delta)^{\alpha-1}f(\delta)d\delta. \tag{39}$$

#### 4.3.1 Application I (yellow virus in red chili plants by FFM)

Using the Mittag-Leffler fractal-fraction operator, the study investigates the yellow virus in red chili plants. Improved fractional order model of the yellow virus is achieved by applying results from fixed point hypothesis. The stability of the Ulam-Hyres model is evaluated using nonlinear analysis. The suggested approach's effectiveness is shown by numerical simulations. Strong tools capable of simulating expected theoretical conditions are employed in this model [145] associated with transmission. This work uses fractional order approaches to investigate the dynamical behavior of the yellow virus in red chili. The yellow virus is becoming more and more of a problem, so it's critical to create plans to halt its spread while preserving immunity. The work makes use of Atangana's unique fractal-fractional operators to observe the unexpected aspects of an issue. The objective of the research is to examine how vaccination affects the yellow virus in the red chilli model by varying the values of $\upsilon_1$ and $\upsilon_2$, which indicate the vaccination effect. The goal of the research is to create methods for stopping the yellow virus from spreading while preserving immunity.

4.3.2 Application II (plant disease model with replanting)

Within fractional calculus, we examine a model of plant disease spread in which sensitive individuals pass through an exposed stage before becoming infectious individuals and whereby illnesses can also be transmitted by exposed plants. The main reason for this delay is that the plant illnesses in the classical example do not impart any knowledge regarding retention and acquisition strategies that influence the spread of a disease. The plant disease model with fractional order in [146] is now viewed as follows.

$$\begin{cases} {}^{ABC}\mathbb{D}_{\blacklozenge}^{\nu} S_1(t) = r(M-N) - \gamma S_1(t) - \frac{a_1}{M} S_1(t) I_1(t) - \alpha S_1(t) + \beta P_1(t), \\ {}^{ABC}\mathbb{D}_{\blacklozenge}^{\nu} P_1(t) = \alpha S_1(t) + \beta P_1(t) - \gamma P_1(t), \\ {}^{ABC}\mathbb{D}_{\blacklozenge}^{\nu} E_1(t) = \frac{a_1}{M} S_1(t) I_1(t) - (\gamma + \alpha_2 + b_1) E_1(t), \\ {}^{ABC}\mathbb{D}_{\blacklozenge}^{\nu} I_1(t) = \alpha_2 E_1(t) - (\gamma + \alpha_3 + b_2 + \eta) I_1(t), \\ {}^{ABC}\mathbb{D}_{\blacklozenge}^{\nu} R_1(t) = \alpha_3 I_1(t) - (\gamma + b_3) R_1(t). \end{cases} \tag{40}$$

4.3.3 Application III (cotton leaf curl virus)

The formula for this is $N_v(t) = X_v + Y_v$. The model took into account the recruiting rate of vulnerable vectors $m_2$ and the transition rate $\alpha_2$ from diseased plants or cotton to infected vectors $(Y_v)$. At $\alpha_1$, the illnesses spread to cotton when sensitive cotton $(S_c)$ is eaten by infected vectors $(Y_v)$. The infections then spread to the sensitive cotton $(S_c)$, which replanted at a pace of $m_1$. Cotton seldom fully recovers from infection and either yields very little or nothing at all. The induced mortality rate, $\beta_1$, and the elimination rate of infected cotton plants from uninfected cotton plants, $\beta_2$, are the parameters used to control the sickness. Additionally, the natural death rates of cotton plants are $d$ and $\psi$. We now view the fractional order plant disease model in [147] as follows.

$$\begin{cases} {}^{ABC}\mathbb{D}_t^{\nu} S_c(t) = m_1 - \alpha_1 S_c Y_v - d S_c, \\ {}^{ABC}\mathbb{D}_t^{\nu} I_c(t) = \alpha_1 S_c Y_v - (d + \beta_1 + \beta_2) I_c, \\ {}^{ABC}\mathbb{D}_t^{\nu} X_v(t) = m_2 - \alpha_2 I_c X_v - \psi X_v, \\ {}^{ABC}\mathbb{D}_t^{\nu} Y_v(t) = \alpha_2 I_c X_v - \psi Y_v. \end{cases} \tag{41}$$

The CLCuV model was employed in the study to classify cotton plants into subgroups that were susceptible to infection. Cotton that is susceptible to infection is denoted as $S_c(t)$, whereas cotton that is vulnerable to infection is $I_c(t)$. There are subclasses of susceptible and infected vectors inside the vector population; the susceptible and infected vectors are represented by the vectors $X_v(t)$ and $Y_v(t)$, accordingly.

## 5 Application of Fractional order derivative for Plant virus model: Future direction

The authors [148] have created a mathematical model to assess the effects of foliar diseases on the dynamics of maize plant inhabitants. Thorough qualitative evaluations of the model's primary components have been approved, indicating that low-cost control approaches can successfully employ it. The authors [149] created a mathematical model to investigate how foliar diseases affect the dynamics of maize plants. They did this by computing asymptotic stability at the equilibrium point of the non-integer system through a system of differential equations for MFD that involves fractional operators and reproduction numbers. A mathematical model for maize foliar disease was published by the authors [150]; it is an improvement over the Collins and Duffy model, which employed a bilinear incidence rate.

This study's primary goal is to apply newly developed fractional derivatives to mathematical modeling and analysis of the maize foliar. The life of the plant is seriously at stake due to the extremely hazardous disease known as maize foliar. Along with a qualitative evaluation of the system, the existence and unique properties of the solution system are verified. Additionally, the actual outcomes of the mathematical model are evaluated using the Atangana-Blaneao derivative. Lastly, the biological observations are verified by numerical simulations. Given the importance of the aforementioned, we intend to focus our effort on these basic questions, utilizing a model that has been carefully designed to account for the constraints of our reaction to the dynamics of maize foliar. First, we demonstrated the epidemic dynamics within a single community with a specific social pattern using a classic method that permits a long incubation period. In this instance, the old model is describe in [148] as follows:

$$\begin{aligned} DS(t) &= \Lambda - P(t)\beta S(t) - \mu_1 S(t); \\ DI(t) &= P(t)\beta S(t) - (\mu_2 + \sigma) I(t); \\ DP(t) &= -\xi P(t) + \sigma I(t). \end{aligned} \tag{42}$$

The following initial circumstances match the system indicated above: $S^0 = S(0)$, $I^0 = I(0)$ and $P^0 = P(0)$.
After the consideration of an integrated control management practices. Model becomes

$$\begin{aligned} DS &= \Lambda - P\beta S - \mu_1 S - \phi S + \tau I; \\ DC &= \phi S - \varepsilon CP - \mu_3 C; \\ DI &= P\beta S + \varepsilon CP - (\mu_2 + \tau) I; \\ DP &= \sigma I - (\xi + \theta) P. \end{aligned} \tag{43}$$

The following initial circumstances match the system indicated above: $S^0 = S(0)$, $C^0 = C(0)$, $I^0 = I(0)$ and $P^0 = P(0)$.

## *5.1 Formulation of pine wilt disease model*

The recovery impact is included in a recently created model for maize foliar, while the prior model only employed the framework. We include a new variable named recover in this new model. A synopsis of the key concepts in this paradigm is provided below; The population at time t is represented by $N(t)$, which is further split into five subclasses. The control population $C(t)$ of maize foliar is subject to worm infection control. Susceptible $S(t)$ is the term used to describe maize foliar that is prone to worm infection. The nematode $I(t)$-infected maize foliar is unable to emit oleoresin into the surrounding environment. The model presupposes a small class of recovered maize foliar $R(t)$. Protected $P(t)$ refers to maize foliar that is protected and measures the pathogens that cause foliar disease up to worm infection. The following are the parameters of the system: $\alpha$ is the transform rate from recover to susceptible, $\phi$ is the transmission rate of susceptible to control, $\tau$ is the rate of transform from infected to susceptible, $\mu_1$ is the rate of natural death of plants, and $\Lambda$ is the recruitment rate into susceptible. Moreover, $\varepsilon$ represents the transmission rate between $P(t)$ and control, $\mu_3$ represents the rate at which plants die as a result of control, and $\eta$ represents the rate at which plants change from control to recover. The system's other parameters are $\sigma$, which indicates the pace at which an infected plant aids in the growth of a protected one, and $\gamma$, which indicates the rate at which an infected plant changes into a recovered one; and $\xi$ and $\theta$ which represent the net decay rate of pathogens and the death rate of $P(t)$, respectively.

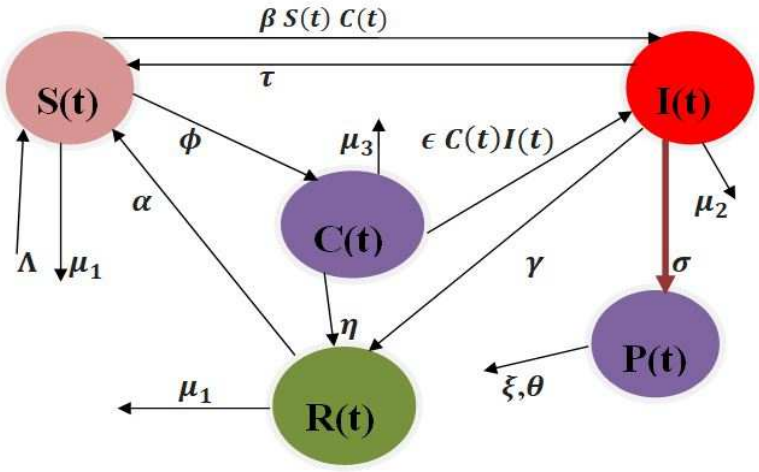


**Fig. 1:** The newly created model is shown in the flow chart.

As a result, the system with the help of flow chart and our created hypothesis shown below as an epidemic model using a host vector and nonlinear incidence

$$\begin{aligned} DS &= \Lambda - C\beta S - \mu_1 S - \phi S + \tau I + \alpha R; \\ DC &= \phi S - \varepsilon CI - (\mu_3 + \eta)C; \\ DI &= C\beta S + \varepsilon CI - (\mu_2 + \tau + \gamma)I; \\ DR &= \eta C + \gamma I - (\alpha + \mu_1)R; \\ DP &= \sigma I - (\xi + \theta)P. \end{aligned} \tag{44}$$

with the following initial conditions: $S^0 = S(0)$, $C^0 = C(0)$, $I^0 = I(0)$, $R^0 = R(0)$ and $P^0 = P(0)$.

Now by applying the fractal fractional derivative definition on above system of differential equations, we get

$$\begin{aligned} {}_0^{FFM}D_t^{\omega,\varpi} S(t) &= \Lambda - \beta SC - \mu_1 S - \phi S + \tau I + \alpha R; \\ {}_0^{FFM}D_t^{\omega,\varpi} C &= \phi S - \varepsilon CI - (\mu_3 + \eta)C; \\ {}_0^{FFM}D_t^{\omega,\varpi} I &= \beta SC + \varepsilon CI - (\mu_2 + \tau + \gamma)I; \\ {}_0^{FFM}D_t^{\omega,\varpi} R &= \eta C + \gamma I - (\alpha + \mu_1)R; \\ {}_0^{FFM}D_t^{\omega,\varpi} P &= \sigma I - (\xi + \theta)P. \end{aligned} \tag{45}$$

The fractal fractional operator of Mittag-Leffler in this case is ${}_0^{FFM}D_t^{\omega,\varpi}$, where $0 < \omega \leq 1$ and $0 < \varpi \leq 1$. The system under description is associated with the initial conditions $S^0 = S(0)$, $C^0 = C(0)$, $I^0 = I(0)$, $R^0 = R(0)$, and $P^0 = P(0)$.

## *5.2 The positive and bounded nature of the solutions*

The research assesses the limits and reasonableness of the circumstances guaranteeing the positive solutions of the suggested model, presuming that they comprise real conditions with pertinent values.

$$\begin{aligned} C(t) &\geq C(0)e^{-(\varepsilon\|I\|_\infty + \mu_3 + \eta)t}, \quad \forall t \geq -\psi \\ I(t) &\geq I(0)e^{-(-\varepsilon\|C\|_\infty + \mu_2 + \tau + \gamma)t}, \quad \forall t \geq -\psi \\ R(t) &\geq R(0)e^{-(\alpha + \mu_1)t}, \quad \forall t \geq -\psi \\ P(t) &\geq P(0)e^{-(\xi + \theta)t}, \quad \forall t \geq -\psi. \end{aligned}$$

Let $D_X$ be the domain of $X$. Define the norm

$$\|X\|_\infty = \sup_{t \in D_X} |X(t)|$$

. With this norm, the function $S(t)$ has;

$$\begin{aligned} {}_0^{FFM}D_t^{\omega,\varpi} S(t) &= \Lambda - \beta SC - \mu_1 S - \phi S + \tau I + \alpha R \geq -\beta SC - \mu_1 S - \phi S \\ &\geq -(\beta C + \mu_1 + \phi)S \geq -(\beta \sup_{t \in D_C} C + \mu_1 + \phi)S = -(\beta\|C\|_\infty + \mu_1 + \phi)S \end{aligned}$$

For ordinary derivative, we have

$$S(t) = S(0)e^{-(\beta\|C\|_\infty + \mu_1 + \phi)t}, \quad \forall t \geq -\psi$$

Positive outcomes utilizing a non-local operator are detailed in the following.

### 5.3 Solutions that work well with a non-local operator

For non-local operators, all outcomes of system (45) are positive if all initial conditions are met.

- With a power law kernel for the Fractal-Fractional operator, we get $\forall t \geq -\psi$.

$$S(t) = S(0)E_a\left(-\varphi^{1-b}(\beta\|C\|_\infty + \mu_1 + \phi)t^a\right),$$
$$C(t) \geq C(0)E_a\left(-\varphi^{1-b}(\varepsilon\|I\|_\infty + \mu_3 + \eta)t^a\right),$$
$$I(t) \geq I(0)E_a\left(-\varphi^{1-b}(-\varepsilon\|C\|_\infty + \mu_2 + \tau + \gamma)t^a\right),$$
$$R(t) \geq R(0)E_a\left(-\varphi^{1-b}(\alpha + \mu_1)t^a\right),$$
$$P(t) \geq P(0)E_a\left(-\varphi^{1-b}(\xi + \theta)t^a\right).$$

where the time component is $\varphi$.

- We obtain $\forall t \geq -\psi$ for a Fractal-Fractional operator with an exponential kernel.

$$S(t) = S(0)exp\left(-\frac{\chi^{1-b}a(\beta\|C\|_\infty + \mu_1 + \phi)t}{\mathscr{M}(a) - (1-a)\left[\beta\|C\|_\infty + \mu_1 + \phi\right]}\right),$$
$$C(t) \geq C(0)exp\left(-\frac{\chi^{1-b}a(\varepsilon\|I\|_\infty + \mu_3 + \eta)t}{\mathscr{M}(a) - (1-a)\left[\varepsilon\|I\|_\infty + \mu_3 + \eta\right]}\right),$$
$$I(t) \geq I(0)exp\left(-\frac{\chi^{1-b}a(-\varepsilon\|C\|_\infty + \mu_2 + \tau + \gamma)t}{\mathscr{M}(a) - (1-a)\left[-\varepsilon\|C\|_\infty + \mu_2 + \tau + \gamma\right]}\right),$$
$$R(t) \geq R(0)exp\left(-\frac{\chi^{1-b}a(\alpha + \mu_1)t}{\mathscr{M}(a) - (1-a)\left[\alpha + \mu_1\right]}\right),$$
$$P(t) \geq P(0)exp\left(-\frac{\chi^{1-b}a(\xi + \theta)t}{\mathscr{M}(a) - (1-a)[\xi + \theta]}\right).$$

- Utilizing a Mittag-Leffler kernel for the fractal-fractional operator, we get $\forall t \geq -\psi$.

$$S(t) = S(0)E_a\left(-\frac{\chi^{1-b}a(\beta\|C\|_\infty + \mu_1 + \phi)t}{\mathscr{AB}(a) - (1-a)\left[\beta\|C\|_\infty + \mu_1 + \phi\right]}\right),$$
$$C(t) \geq C(0)E_a\left(-\frac{\chi^{1-b}a(\varepsilon\|I\|_\infty + \mu_3 + \eta)t}{\mathscr{AB}(a) - (1-a)\left[\varepsilon\|I\|_\infty + \mu_3 + \eta\right]}\right),$$
$$I(t) \geq I(0)E_a\left(-\frac{\chi^{1-b}a(-\varepsilon\|C\|_\infty + \mu_2 + \tau + \gamma)t}{\mathscr{AB}(a) - (1-a)\left[-\varepsilon\|C\|_\infty + \mu_2 + \tau + \gamma\right]}\right),$$
$$R(t) \geq R(0)E_a\left(-\frac{\chi^{1-b}a(\alpha + \mu_1)t}{\mathscr{AB}(a) - (1-a)\left[\alpha + \mu_1\right]}\right),$$
$$P(t) \geq P(0)E_a\left(-\frac{\chi^{1-b}a(\xi + \theta)t}{\mathscr{AB}(a) - (1-a)[\xi + \theta]}\right).$$

### 5.4 Model's Reproductive Number and Equilibrium Point

The disease-free equilibrium for this model 45 is $E_1(S,C,I,R,P)$., where

$$S = \frac{\Lambda(\alpha + \mu_1)(\eta + \mu_3)}{\alpha\eta\mu_1 + \alpha_1\mu_1\mu_3 + \alpha\mu_3\phi + \eta\mu_1^2 + \eta\mu_1\phi + \mu_1^2\mu_3 + \mu_1\mu_3\phi}$$
$$C = \frac{\Lambda\phi(\alpha + \mu_1)}{\alpha\eta\mu_1 + \alpha_1\mu_1\mu_3 + \alpha\mu_3\phi + \eta\mu_1^2 + \eta\mu_1\phi + \mu_1^2\mu_3 + \mu_1\mu_3\phi}$$
$$I = 0$$
$$R = \frac{\eta\Lambda\phi}{\alpha\eta\mu_1 + \alpha_1\mu_1\mu_3 + \alpha\mu_3\phi + \eta\mu_1^2 + \eta\mu_1\phi + \mu_1^2\mu_3 + \mu_1\mu_3\phi}$$
$$P = 0$$

together with the pandemic point of equilibrium, which are as follows: $E_2(S^*, C^*, I^*, R^*, P^*)$ and reproductive number is

$$R_0 = \frac{1}{2\phi(\alpha+\mu_1)(\eta+\mu_3)(\theta+\xi)\left(\alpha\mu_1+\mu_1^2+\mu_1\phi\right)(\gamma+\mu_2+\tau)}\Big[\alpha^2\beta\eta\Lambda\sigma\phi+\alpha^2\beta\Lambda\mu_3\sigma\phi$$
$$+\sqrt{\Lambda}\sqrt{\sigma}\phi(\alpha+\mu_1)^{3/2}\sqrt{\eta+\mu_3}\sqrt{\mathfrak{A}}+2\alpha\beta\eta\Lambda\mu_1\sigma\phi+2\alpha\beta\Lambda\mu_1\mu_3\sigma\phi+\beta\eta\Lambda\mu_1^2\sigma\phi+\beta\Lambda\mu_1^2\mu_3\sigma\phi\Big];$$

where

$$\mathfrak{A} = \alpha^2\beta\eta\Lambda\sigma\phi+\alpha^2\beta\Lambda\mu_3\sigma\phi+\sqrt{\Lambda}\sqrt{\sigma}\phi(\alpha+\mu_1)^{3/2}\sqrt{\eta+\mu_3}\sqrt{\mathfrak{A}_1}+2\alpha\beta\eta\Lambda\mu_1\sigma\phi+$$
$$2\alpha\beta\Lambda\mu_1\mu_3\sigma\phi+\beta\eta\Lambda\mu_1^2\sigma\phi+\beta\Lambda\mu_1^2\mu_3\sigma\phi,$$

$$\mathfrak{A}_1 = \alpha\beta^2\eta\Lambda\sigma+\alpha\beta^2\Lambda\mu_3\sigma+4\alpha\gamma\theta\mu_1\varepsilon\phi+4\alpha\gamma\mu_1\xi\varepsilon\phi+4\alpha\theta\mu_1\mu_2\varepsilon\phi+4\alpha\theta\mu_1\tau\varepsilon\phi+4\alpha\mu_1\mu_2\xi\varepsilon\phi$$
$$+4\alpha\mu_1\xi\tau\varepsilon\phi+\beta^2\eta\Lambda\mu_1\sigma+\beta^2\Lambda\mu_1\mu_3\sigma+4\gamma\theta\mu_1^2\varepsilon\phi+4\gamma\theta\mu_1\varepsilon\phi^2+4\gamma\mu_1^2\xi\varepsilon\phi+4\gamma\mu_1\xi\varepsilon\phi^2$$
$$+4\theta\mu_1^2\mu_2\varepsilon\phi+4\theta\mu_1^2\tau\varepsilon\phi+4\theta\mu_1\mu_2\varepsilon\phi^2+4\theta\mu_1\tau\varepsilon\phi^2+4\mu_1^2\mu_2\xi\varepsilon\phi+4\mu_1^2\xi\tau\varepsilon\phi+4\mu_1\mu_2\xi\varepsilon\phi^2$$
$$+4\mu_1\xi\tau\varepsilon\phi^2.$$

### *5.5 Solutions of the Model that are Positive and Bounded*

We prove the constructed model's positivity and boundedness in this section.

**Theorem 1:** In addition to the initial condition, the suggested maize foliar disease model Eqn. 45 in $R_+^5$ is distinct and confined.

**Proof:**

We possess

$$\begin{aligned}
&{}_0^{FFM}D_t^{\omega,\varpi}S = \Lambda+\tau I+\alpha R \geq 0;\\
&{}_0^{FFM}D_t^{\omega,\varpi}C = \phi S \geq 0;\\
&{}_0^{FFM}D_t^{\omega,\varpi}I = \beta SC+\varepsilon CI \geq 0;\\
&{}_0^{FFM}D_t^{\omega,\varpi}R = \eta C+\gamma I \geq 0;\\
&{}_0^{FFM}D_t^{\omega,\varpi}P = \sigma I \geq 0.
\end{aligned} \tag{46}$$

Equation 45 states that our obtained solution cannot escape from the hyperplane if $(S(0), C(0), I(0), R(0), P(0)) \in R_+^5$. This demonstrates that a positive invariant is achieved in the $R_5^+$ domain.

**Theorem. 2:** For each $t > 0$, $S(0)$, $C(0)$, $I(0)$, $R(0)$, and $P(0)$ are all positive if the answers to a system of equations are $S$, $C$, $I$, $R$, and $P$.

**Proof:** To demonstrate why your responses are good—they portray positive values in real-world scenarios—let's begin with a fundamental examination. We look at the requirements in this part to make sure the suggested model's solutions are positive. Start by using the $S$ class. The first formula provides

$$S \geq S(0)e^{-(\beta C+\mu_1+\phi)t}+e^{-(\beta C+\mu_1+\phi)t}\rho_1 \geq 0.$$

The remaining formulas will be

$$\begin{aligned}
C &\geq C(0)e^{-(\varepsilon I+\mu_3+\eta))t}+e^{-(\varepsilon I+\mu_3+\eta)t}\rho_2 \geq 0,\\
I &\geq I(0)e^{-(\mu_2+\tau+\gamma)t}+e^{-(\mu_2+\tau+\gamma)t}\rho_3 \geq 0,\\
R &\geq R(0)e^{-(\alpha+\mu_1)t}+e^{-(\alpha+\mu_1)t}\rho_4 \geq 0,\\
P &\geq P(0)e^{-(\xi+\theta)t}+e^{-(\xi+\theta)t}\rho_5 \geq 0,
\end{aligned}$$

Where

$$\rho_1 = \int_0^{t^*} [\Lambda + \tau I + \alpha R] e^{(\beta P + \mu_1 + \phi)\psi} d\psi,$$
$$\rho_2 = \int_0^{t^*} \phi S e^{(\varepsilon I + \mu_3 + \eta)\psi} d\psi,$$
$$\rho_3 = \int_0^{t^*} [\beta SC + \varepsilon CI] e^{(\mu_2 + \tau + \gamma)\psi} d\psi,$$
$$\rho_4 = \int_0^{t^*} [\eta C + \gamma I] e^{(\alpha + \mu_1)\psi} d\psi,$$
$$\rho_5 = \int_0^{t^*} \sigma I e^{(\xi + \theta)\psi} d\psi.$$

### *5.6 Effects of Global Derivatives on Solution Uniqueness and Exitance*

The most often used integral in the literature is generally acknowledged to be the Riemann-Stieltjes integral. If

$$Y(a) = \int y(a) dx.$$

Here is an expression for the Riemann-Stieltjes integral.

$$Y_g(a) = \int y(a) dg x.$$

Regarding $g(a)$, the global derivative of $y(a)$ is

$$D_g y(a) = \lim_{h \to 0} \frac{y(a+h) - y(a)}{g(a+h) - g(a)}.$$

When the numerator and denominator of the aforementioned functions differentiate, we obtain

$$D_g y(a) = \lim_{h \to 0} \frac{y'(a)}{g'(a)}.$$

Now that we have assumed that $g'(a) \neq 0$, we will investigate the impact on the maize foliar virus by using the global derivative in place of the classical derivative $\forall a \in \mathbb{D}'_g$.

$$\begin{aligned}
D_g S &= \Lambda - \beta SC - \mu_1 S - \phi S + \tau I + \alpha R; \\
D_g C &= \phi S - \varepsilon CI - (\mu_3 + \eta) C; \\
D_g I &= \beta SC + \varepsilon CI - (\mu_2 + \tau + \gamma) I; \\
D_g R &= \eta C + \gamma I - (\alpha + \mu_1) R; \\
D_g P &= \sigma I - (\xi + \theta) P.
\end{aligned}$$

Let's assume for the sake of hygiene that $g$ is differentiable.

$$\begin{aligned}
S' &= g'[\Lambda - \beta SC - \mu_1 S - \phi S + \tau I + \alpha R]; \\
C' &= g'[\phi S - \varepsilon CI - (\mu_3 + \eta) C]; \\
I' &= g'[\beta SC + \varepsilon CI - (\mu_2 + \tau + \gamma) I]; \\
R' &= g'[\eta C + \gamma I - (\alpha + \mu_1) R]; \\
P' &= g'[\sigma I - (\xi + \theta) P].
\end{aligned}$$

A particular result will be obtained if the function $g$ is chosen appropriately. Fractal movement will be seen, for example, if $g = t^{\zeta}$, where $\zeta$ is a real number. The conditions that required us to act were

$$\|g'\|_{\infty} = \sup_{t \in D'_g} g < N.$$

The developed system's unique solution is illustrated in the example below.

$$\begin{aligned}
S' &= g'[\Lambda - \beta SC - \mu_1 S - \phi S + \tau I + \alpha R];\\
C' &= g'[\phi S - \varepsilon CI - (\mu_3 + \eta)C];\\
I' &= g'[\beta SC + \varepsilon CI - (\mu_2 + \tau + \gamma)I];\\
R' &= g'[\eta C + \gamma I - (\alpha + \mu_1)R];\\
P' &= g'[\sigma I - (\xi + \theta)P].
\end{aligned}$$

Where

$$\xi = S, C, I, R, P$$

The following two prerequisites need to be confirmed.

1. $|J(t,S,C,I,R,P)| < K(1+|S|^2)$
2. $\forall S_1, S_2$, we have

$$\|J(t,S_1,C,I,R,P) - J(t,S_2,C,I,R,P)\| < k\|S_1 - S_2\|_\infty.$$

Initially,

$$\begin{aligned}
|J_1(t,\xi)|^2 &= |g'[\Lambda - \beta SC - \mu_1 S - \phi S + \tau I + \alpha R]|^2\\
&= |g'|^2\,|[\Lambda - \beta SC - \mu_1 S - \phi S + \tau I + \alpha R]|^2\\
&\le 2|g'|^2[|\Lambda|^2 + |-\beta SC - \mu_1 S - \phi S + \tau I + \alpha R|^2]\\
&\le 2|g'|^2[|\Lambda|^2 + 2|\tau I|^2 + 2|\alpha R - \beta SC - \mu_1 S - \phi S|^2]\\
&\le 2|g'|^2[|\Lambda|^2 + 2|\tau I|^2 + 4|\alpha R| + 4|(\beta C + \mu_1 + \phi)S|^2]\\
&= 2|g'|^2 2|\Lambda|^2 + 4|\tau I|^2 + 8|\alpha R| + 8|(\beta C + \mu_1 + \phi)|^2|S|^2]\\
&= 2|g'|^2 2|\Lambda|^2 + 4|\tau I|^2 + 8|\alpha R|[1 + \frac{(\beta C + \mu_1 + \phi)|^2}{2|\Lambda|^2 + 4|\tau I|^2 + 8|\alpha R|}|S|^2]\\
&< k_1(1+|S|^2).
\end{aligned}$$

Under the conditions

$$\frac{(\beta C + \mu_1 + \phi)|^2}{2|\Lambda|^2 + 4|\tau I|^2 + 8|\alpha R|} < 1,$$

where

$$k_1 = 2|g'|^2 2|\Lambda|^2 + 4|\tau I|^2 + 8|\alpha R|.$$

$$\begin{aligned}
|J_2(t,\xi)|^2 &= |g'[\phi S - \varepsilon CI - (\mu_3 + \eta)C]|^2\\
&= |g'|^2|[\phi S - \varepsilon CI - (\mu_3 + \eta)C]|^2\\
&\le 2|g'|^2[|\phi S|^2 + |-(\varepsilon I + (\mu_3 + \eta))C|^2]\\
&= 2|g'|^2[|\phi S|^2 + |(\varepsilon I + \mu_3 + \eta)C|^2]\\
&= 2|g'|^2|\phi S|^2[1 + \frac{(\varepsilon I + \mu_3 + \eta)^2}{|\phi S|^2}|C|^2]\\
&< k_2(1+|C|^2).
\end{aligned}$$

Under the conditions

$$\frac{(\varepsilon I + \mu_3 + \eta)^2}{|\phi S|^2} < 1,$$

where

$$k_2 = 2|g'|^2|\phi S|^2.$$

$$\begin{aligned}
|J_3(t,\xi)|^2 &= |g'[\beta SC+\varepsilon CI-(\mu_2+\tau+\gamma)I]|^2\\
&= |g'|^2|[\beta SC+\varepsilon CI-(\mu_2+\tau+\gamma)I]|^2\\
&\leq 2|g'|^2[|\beta SC|^2+|\varepsilon CI-(\mu_2+\tau+\gamma)I|^2]\\
&\leq 2|g'|^2[|\beta SC|^2+2|\varepsilon CI|^2+2|(\mu_2+\tau+\gamma)I|^2]\\
&= 2|g'|^2[|\beta SC|^2+4|\varepsilon CI|^2+4|(\mu_2+\tau+\gamma)I|^2]\\
&= 2|g'|^2[|\beta SC|^2+4|\varepsilon CI|^2][1+\frac{4(\mu_2+\tau+\gamma)^2}{|\beta SP|^2+4|\varepsilon CP|^2}|I|^2]\\
&< k_3(1+|I|^2)
\end{aligned}$$

Under the conditions

$$\frac{4(\mu_2+\tau+\gamma)^2}{|\beta SC|^2+4|\varepsilon CI|^2}<1$$

where

$$k_3 = 2|g'|^2|\beta SC|^2+4|\varepsilon CI|^2.$$

$$\begin{aligned}
|J_4(t,\xi)|^2 &= |g'[\eta C+\gamma I-(\alpha+\mu_1)R]|^2\\
&= |g'|^2[|\eta C+\gamma I-(\alpha+\mu_1)R|^2]\\
&\leq 2|g'|^2[|\eta C|^2+|\gamma I-(\alpha+\mu_1)R|^2]\\
&\leq 2|g'|^2[|\eta C|^2+2|\gamma I|^2+2|(\alpha+\mu_1)R|^2]\\
&= 2|g'|^2[|\eta C|^2+2|\gamma I|^2+2|(\alpha+\mu_1)|^2|R|^2]\\
&= 2|g'|^2(|\eta C|^2+2|\gamma I|^2)[1+\frac{2|(\alpha+\mu_1)|^2}{|\eta C|^2+2|\gamma I|^2}|R|^2]\\
&< k_4(1+|R|^2).
\end{aligned}$$

Under the conditions

$$\frac{2|(\alpha+\mu_1)|^2}{|\eta C|^2+2|\gamma I|^2}<1,$$

where

$$k_4 = 2|g'|^2(|\eta C|^2+2|\gamma I|^2).$$

$$\begin{aligned}
|J_5(t,\xi)|^2 &= |g'[\sigma I-(\xi+\theta)P]|^2\\
&= |g'|^2[|\sigma I-(\xi+\theta)P|^2]\\
&\leq 2|g'|^2[|\sigma I|^2+|(\xi+\theta)P|^2]\\
&= 2|g'|^2[|\sigma I|^2+|(\xi+\theta)|^2|P|^2]\\
&= 2|g'|^2|\sigma I|^2[1+\frac{|(\xi+\theta)|^2}{|\sigma I|^2}|P|^2]\\
&< k_5(1+|P|^2).
\end{aligned}$$

Under the conditions

$$\frac{|(\xi+\theta)|^2}{|\sigma I|^2}<1,$$

where

$$k_5 = 2|g'|^2|\sigma I|^2.$$

The requirements for linear growth are thereby met.

Furthermore, confirm Lipschitz's state using the following method. When

$$\begin{aligned}|J_1(t,S_1,C,I,R,P)-J_1(t,S_2,C,I,R,P|^2 &= (|-(\beta C+\mu_1+\phi)|^2)|S_1-S_2|^2\\ &= (|(\beta C+\mu_1+\phi)|^2)|S_1-S_2|^2\\ &\leq \left\{2|\beta C|^2+2|(\mu_1+\phi)|^2\right\}|S_1-S_2|^2\\ &= \left\{2|\beta|^2|C|^2+2|(\mu_1+\phi)|^2\right\}|S_1-S_2|^2\\ &\leq \left\{2|\beta|^2\sup_{t\in D_C}|C|^2+2|(\mu_1+\phi)|^2\right\}\sup_{t\in D_S}|S_1-S_2|^2\\ &\leq \left\{2|\beta|^2\|C\|_\infty+2|(\mu_1+\phi)|^2\right\}\|S_1-S_2\|_\infty\\ &\leq \overline{k}_1\|S_1-S_2\|_\infty,\end{aligned}$$

where

$\overline{k}_1 = 2|\beta|^2\|C\|_\infty+2|(\mu_1+\phi)|^2.$

If

$$\begin{aligned}|J_2(t,S,C_1,I,R,P)-J_2(t,S,C_2,I,R,P)|^2 &= |-(\varepsilon I+\mu_3+\eta)C_1-C_2|^2\\ &\leq \left\{2|\varepsilon I|^2+2|(\mu_3+\eta)|^2\right\}|C_1-C_2|^2\\ &= \left\{|\varepsilon|^2|I|^2+|(\mu_3+\eta)|^2\right\}|C_1-C_2|^2\\ &\leq \left\{|\varepsilon|^2\sup_{t\in D_I}|I|^2+|(\mu_3+\eta)|^2\right\}\sup_{t\in D_C}|C_1-C_2|^2\\ &= \left\{|\varepsilon|^2\|I\|_\infty+|(\mu_3+\eta)|^2\right\}\|C_1-C_2\|_\infty\\ &\leq \overline{k}_2\|C_1-C_2\|_\infty,\end{aligned}$$

where

$\overline{k}_2 = \left\{|\varepsilon|^2\|I\|_\infty+|(\mu_3+\eta)|^2\right\}.$

If

$$\begin{aligned}|J_3(t,S,C,I_1,R,P)-J_3(t,S,C,I_2,R,P)|^2 &= |-(\mu_2+\tau+\gamma)I_1-I_2|^2\\ &\leq |(\mu_2+\tau+\gamma)|^2\sup_{t\in D_I}|I_1-I_2|^2\\ &= |(\mu_2+\tau+\gamma)|^2\|I_1-I_2\|_\infty\\ &\leq \overline{k}_3\|I_1-I_2\|_\infty,\end{aligned}$$

where

$\overline{k}_3 = |(\mu_2+\tau+\gamma)|^2.$

If

$$\begin{aligned}|J_4(t,S,C,I,R_1,P)-J_4(t,S,C,I,R_2,P)|^2 &= |-(\alpha+\mu_1)(R_1-R_2)|^2\\ &= |-(\alpha+\mu_1)|^2|(R_1-R_2)|^2\\ &\leq |(\alpha+\mu_1)|^2\sup_{t\in D_R}|(R_1-R_2)|^2\\ &\leq \overline{k}_4\|R_1-R_2\|_\infty,\end{aligned}$$

where

$\overline{k}_4 = |(\alpha+\mu_1)|^2.$

If

$$\begin{aligned}|J_5(t,S,C,I,R,P_1)-J_5(t,S,C,I,R,P_2)|^2 &= |-(\xi+\theta)(P_1-P_2)|^2\\ &= |-(\xi+\theta)|^2|(P_1-P_2)|^2\\ &\leq |(\xi+\theta)|^2\sup_{t\in D_P}|(P_1-P_2)|^2\\ &\leq \overline{k}_5\|P_1-P_2\|_\infty,\end{aligned}$$

where

$\overline{k}_5 = |(\xi+\theta)|^2$.

Then, system 45 has a specific solution given the condition.

$$\max\left[\frac{(\beta P+\mu_1+\phi)|^2}{2|\Lambda|^2+4|\tau I|^2+8|\alpha R|}, \frac{(\varepsilon P+\mu_3+\eta)^2}{|\phi S|^2}, \frac{4(\mu_2+\tau+\gamma)^2}{|\beta SP|^2+4|\varepsilon CP|^2}, \frac{2|(\alpha+\mu_1)|^2}{|\eta C|^2+2|\gamma I|^2}, \frac{|(\xi+\theta)|^2}{|\sigma I|^2}\right] < 1.$$

## *5.7 Global Stability for Newly Generated Model*

We apply Lyapunov's technique and LaSalle's concept of invariance to investigate global stability and determine the conditions for disease cure.

## *5.8 Lyapunov's First Derivative*

**Theorem. 3:** Assuming that $R_0 < 1$, the model's endemismically stable states are globally asymptotically stable.

**Proof:** The Lyapunov function is expressed as follows.

$$L(S^*,C^*,I^*,R^*,P^*) = (S-S^*-S^*log\frac{S^*}{S})+(C-C^*-C^*log\frac{C^*}{C})+(I-(1+log\frac{I^*}{I})I^*)+$$
$$(R-(1+log\frac{R^*}{R})R^*)+(P-P^*-P^*log\frac{P^*}{P}).$$

We accomplish this by using both sides of the fractal fractional derivative.

$${}_0^{FFM}D_t^{\omega,\varpi}L = \left(\frac{S-S^*}{S}\right){}_0^{FFM}D_t^{\omega,\varpi}S+\left(\frac{C-C^*}{C}\right){}_0^{FFM}D_t^{\omega,\varpi}C+\left(\frac{I-I^*}{I}\right){}_0^{FFM}D_t^{\omega,\varpi}I$$
$$+\left(\frac{R-R^*}{R}\right){}_0^{FFM}D_t^{\omega,\varpi}R+\left(\frac{P-P^*}{P}\right){}_0^{FFM}D_t^{\omega,\varpi}P.$$

We get

$${}_0^{FFM}D_t^{\omega,\varpi}L = \left(\frac{S-S^*}{S}\right)(\Lambda-\beta SC-\mu_1 S-\phi S+\tau I+\alpha R)+\left(\frac{C-C^*}{C}\right)(\phi S-\varepsilon CI-(\mu_3+\eta)C)$$
$$+\left(\frac{I-I^*}{I}\right)(\beta SC+\varepsilon CI-(\mu_2+\tau+\gamma)I)+\left(\frac{R-R^*}{R}\right)(\eta C+\gamma I-(\alpha+\mu_1)R)$$
$$+\left(\frac{P-P^*}{P}\right)(\sigma I-(\xi+\theta)P).$$

Putting $S = S-S^*$, $C = C-C^*$, $I = I-I^*$, $R = R-R^*$, $P = P-P^*$.

$${}_0^{FFM}D_t^{\omega,\varpi}L = \left(\frac{S-S^*}{S}\right)(\Lambda-\beta(S-S^*)(C-C^*)-\mu_1(S-S^*)-\phi(S-S^*)+\tau(I-I^*)+\alpha(R-R^*))$$
$$+\left(\frac{C-C^*}{C}\right)(\phi(S-S^*)-\varepsilon(C-C^*)(I-I^*)-(\mu_3+\eta)(C-C^*))$$
$$+\left(\frac{I-I^*}{I}\right)(\beta(S-S^*)(C-C^*)\varepsilon(C-C^*)(I-I^*)-(\mu_2+\tau+\gamma)(I-I^*))$$
$$+\left(\frac{R-R^*}{R}\right)(\eta(C-C^*)+\gamma(I-I^*)-(\alpha+\mu_1)(R-R^*))$$
$$+\left(1-\frac{P^*}{P}\right)(\sigma(I-I^*)-(\xi+\theta)(P-P^*)).$$

It also can be organize that

$$
\begin{aligned}
{}_0^{FFM}D_t^{\omega,\varpi}L = \Lambda &- \frac{\Lambda S^*}{S} - \frac{\beta}{S}(S-S^*)^2C + \frac{\beta}{S}(S-S^*)^2C^* - \frac{\mu_1}{S}(S-S^*)^2 - \frac{\phi}{S}(S-S^*)^2 + \tau I - \tau I^* \\
&- \frac{S^*}{S}\tau I + \frac{S^*}{S}\tau I^* + \alpha R - \alpha R^* - \frac{S^*}{S}\alpha R + \frac{S^*}{S}\alpha R^* + \phi S - \phi S^* - \frac{C^*}{C}\phi + \frac{C^*}{C}\phi S^* \\
&- \frac{\varepsilon}{C}(C-C^*)^2 I + \frac{\varepsilon}{C}(C-C^*)^2 I^* - \frac{(\mu_3+\eta)}{C}(C-C^*)^2 + \beta SC - \beta S^*C - \beta SC^* \\
&+ \beta S^*C^* - \frac{I^*}{I}\beta SC + \frac{I^*}{I}\beta S^*C + \frac{I^*}{I}\beta SC^* - \frac{I^*}{I}\beta S^*C^* + \varepsilon CI - \varepsilon C^*I - \varepsilon CI^* + \varepsilon C^*I^* \\
&- \frac{I^*}{I}\varepsilon CI + \frac{I^*}{I}\varepsilon C^*I + \frac{I^*}{I}\varepsilon CI^* - \frac{I^*}{I}\varepsilon C^*I^* - \frac{(\mu_2+\tau+\gamma)}{I}(I-I^*)^2 + \eta C - \eta C^* \\
&- \eta\frac{R^*}{R}C + \eta\frac{R^*}{R}C^* + \gamma I - \gamma I^* - \gamma\frac{R^*}{R}I + \gamma\frac{R^*}{R}I^* - \frac{(\alpha+\mu_1)}{R}(R-R^*)^2 + \sigma I - \sigma I^* \\
&- \sigma\frac{P^*}{P}I + \sigma\frac{P^*}{P}I^* - \frac{(\xi+\theta)}{P}(P-P^*)^2.
\end{aligned}
$$

Which can be written as

$$
{}_0^{FFM}D_t^{\omega,\varpi}L = M - N. \tag{47}
$$

Where

$$
\begin{aligned}
M = \Lambda &+ \frac{\beta}{S}(S-S^*)^2C^* + \tau I - \tau I^* + \frac{S^*}{S}\tau I^* + \alpha R + \frac{S^*}{S}\alpha R^* + \phi S + \frac{C^*}{C}\phi S^* + \frac{\varepsilon}{C}(C-C^*)^2 I^* \\
&+ \beta SC + \beta S^*C^* + \frac{I^*}{I}\beta S^*C + \frac{I^*}{I}\beta SC^* + \varepsilon CI + \varepsilon C^*I^* + \frac{I^*}{I}\varepsilon C^*I + \frac{I^*}{I}\varepsilon CI^* + \eta C + \eta\frac{R^*}{R}C^* \\
&+ \gamma I + \gamma\frac{R^*}{R}I^* + \sigma I + \sigma\frac{P^*}{P}I^*,
\end{aligned}
$$

and

$$
\begin{aligned}
N = &\frac{\Lambda S^*}{S} + \frac{\beta}{S}(S-S^*)^2C + \frac{\mu_1}{S}(S-S^*)^2 + \frac{\phi}{S}(S-S^*)^2 + \tau I^* + \frac{S^*}{S}\tau I + \alpha R^* + \frac{S^*}{S}\alpha R + \phi S^* + \frac{C^*}{C}\phi \\
&+ \frac{\varepsilon}{C}(C-C^*)^2 I + \frac{(\mu_3+\eta)}{C}(C-C^*)^2 + \beta S^*C + \beta SC^* + \frac{I^*}{I}\beta SC + \frac{I^*}{I}\beta S^*C^* + \varepsilon C^*C + \varepsilon CC^* + \frac{I^*}{I}\varepsilon CI \\
&+ \frac{I^*}{I}\varepsilon C^*I^* + \frac{(\mu_2+\tau+\gamma)}{I}(I-I^*)^2 + \eta C^* + \eta\frac{R^*}{R}C + \gamma I^* + \gamma\frac{R^*}{R}I + \frac{(\alpha+\mu_1)}{R}(R-R^*)^2 + \sigma I^* \\
&+ \sigma\frac{P^*}{P}I + \frac{(\xi+\theta)}{P}(P-P^*)^2.
\end{aligned}
$$

In summary, we find that when $M < N$, this results in ${}_0^{FFM}D_t^{\omega,\varpi}L < 0$; on the other hand, when $S = S^*$, $C = C^*$, $I = I^*$, $R = R^*$, $P = P^*$, then

$$
0 = M - N \quad \Rightarrow {}_0^{FFM}D_t^{\omega,\varpi}L = 0.
$$

We can see that $\{(S^*, C^*, I^*, R^*, P^*, I_v^*) \in \mathbb{R}_5^+ : {}_0^{FFM}D_t^{\omega,\varpi}L = 0\}$.

The model is globally uniformly stable in accordance with Lasalles' concept of invariance.

### *5.9 Numerical Algorithm with Fractal Fractional Operator*

We will now use the numerical approach to find a solution for our newly developed model, which is represented by equation 45. In the present case, we substitute the ML kernel for the classical derivative operator. We'll also employ the version with a flexible order. We state the equation 45 as follows for clarity:

$$
\begin{aligned}
&{}_0^{FFM}D_t^{\omega,\varpi}S = \Lambda - \beta SC - \mu_1 S - \phi S + \tau I + \alpha R = S_1(t,\pi);\\
&{}_0^{FFM}D_t^{\omega,\varpi}C = \phi S - \varepsilon CI - (\mu_3+\eta)C = C_1(t,\pi);\\
&{}_0^{FFM}D_t^{\omega,\varpi}I = \beta SC + \varepsilon CI - (\mu_2+\tau+\gamma)I = I_1(t,\pi);\\
&{}_0^{FFM}D_t^{\omega,\varpi}R = \eta C + \gamma I - (\alpha+\mu_1)R = R_1(t,\pi);\\
&{}_0^{FFM}D_t^{\omega,\varpi}P = \sigma I - (\xi+\theta)P = P_1(t,\pi).
\end{aligned}
$$

Following the application of the ML kernel and the fractal-fractional integral, we find the following outcomes.

$$
\begin{aligned}
S(t_{k+1}) &= S_0 + \frac{1-\omega}{AB(\omega)}t_k^{1-\varpi}S_1(t_k,S(t_k),C(t_k),I(t_k),R(t_k),P(t_k)) + \hbar\sum_{i=2}^{k}\int_{t_i}^{t_{i+1}} S_1(t,\pi)\varsigma^{1-\varpi}(t_{k+1}-\varsigma)^{\omega-1}d\varsigma,\\
C(t_{k+1}) &= C_0 + \frac{1-\omega}{AB(\omega)}t_k^{1-\varpi}C_1(t_k,S(t_k),C(t_k),I(t_k),R(t_k),P(t_k)) + \hbar\sum_{i=2}^{k}\int_{t_i}^{t_{i+1}} C_1(t,\pi)\varsigma^{1-\varpi}(t_{k+1}-\varsigma)^{\omega-1}d\varsigma,\\
I(t_{k+1}) &= I_0 + \frac{1-\omega}{AB(\omega)}t_k^{1-\varpi}I_1(t_k,S(t_k),C(t_k),I(t_k),R(t_k),P(t_k)) + \hbar\sum_{i=2}^{k}\int_{t_i}^{t_{i+1}} I_1(t,\pi)\varsigma^{1-\varpi}(t_{k+1}-\varsigma)^{\omega-1}d\varsigma,\\
R(t_{k+1}) &= R_0 + \frac{1-\omega}{AB(\omega)}t_k^{1-\varpi}R_1(t_k,S(t_k),C(t_k),I(t_k),R(t_k),P(t_k)) + \hbar\sum_{i=2}^{k}\int_{t_i}^{t_{i+1}} R_1(t,\pi)\varsigma^{1-\varpi}(t_{k+1}-\varsigma)^{\omega-1}d\varsigma,\\
P(t_{k+1}) &= P_0 + \frac{1-\omega}{AB(\omega)}t_k^{1-\varpi}P_1(t_k,S(t_k),C(t_k),I(t_k),R(t_k),P(t_k)) + \hbar\sum_{i=2}^{k}\int_{t_i}^{t_{i+1}} P_1(t,\pi)\varsigma^{1-\varpi}(t_{k+1}-\varsigma)^{\omega-1}d\varsigma.
\end{aligned}
$$

where $\pi = S,C,I,R,P$ and $\hbar = \frac{\omega}{AB(\omega)\Gamma(\omega)}$. Here, we recall the Newton polynomial:

$$
\begin{aligned}
&\mathscr{A}(t,\pi) && (48)\\
&\simeq \mathscr{A}(t_{k-2},S_{k-2},C_{k-2},I_{k-2},R_{k-2},\mathscr{A}_{k-2}) + \frac{1}{\triangle t}\Big\{P(t_{k-1},S_{k-1},C_{k-1},I_{k-21},R_{k-1},P_{k-1}) && (49)\\
&-\mathscr{A}(t_{k-2},S_{k-2},C_{k-2},I_{k-2},R_{k-2},P_{k-2})\Big\}\times(\varsigma-t_{k-2})\\
&+\frac{1}{2\triangle t^2}\Big\{\mathscr{A}(t,S_k,C_k,I_k,R_k,P_k) - 2\mathscr{A}(t_{k-1},S_{k-1},C_{k-1},I_{k-21},R_{k-1},P_{k-1})\\
&-\mathscr{A}(t_{k-2},S_{k-2},C_{k-2},I_{k-2},R_{k-2},P_{k-2})\Big\}\times(\varsigma-t_{k-2})(\varsigma-t_{k-1}).
\end{aligned}
$$

Substituting (48) into above equations, we find

$$
\begin{aligned}
S_{k+1} &= S_0 + \frac{1-\omega}{AB(\omega)}t_k^{1-\varpi}S_1(t_k,S(t_k),C(t_k),I(t_k),R(t_k),P(t_k)) + \hbar\sum_{i=2}^{k}S_1[t_{i-2},S^{i-2},C^{i-2},I^{i-2},R^{i-2},P^{i-2}]t_{i-2}^{1-\varpi}\\
&\times\int_{t_i}^{t_{i+1}}(t_{k+1}-\varsigma)^{\omega-1}d\varsigma + \hbar\sum_{i=2}^{k}\frac{1}{\triangle t}\Big\{t_{i-1}^{1-\varpi}S_1(t_{i-1},S^{i-1},C^{i-1},I^{i-1},R^{i-1},P^{i-1}) - t_{i-2}^{1-\varpi}S_1[t_{i-2},S^{i-2},C^{i-2},\\
&I^{i-2},R^{i-2},P^{i-2}]\Big\}\times\int_{t_i}^{t_{i+1}}(\varsigma-t_{i-2})(t_{k+1}-\varsigma)^{\omega-1}d\varsigma + \hbar\sum_{i=2}^{k}\frac{1}{2\triangle t^2}\Big\{t_i^{1-\varpi}S_1[t_i,S^i,C^i,I^i,R^i,P^i] -\\
&2t_{i-1}^{1-\varpi}S_1(t_{i-1},S^{i-1},C^{i-1},I^{i-1},R^{i-1},P^{i-1}) + t_{i-2}^{1-\varpi}S_1[t_{i-2},S^{i-2},C^{i-2},I^{i-2},R^{i-2},P^{i-2}]\Big\}\\
&\times\int_{t_i}^{t_{i+1}}(\varsigma-t_{i-2})(\varsigma-t_{i-1})(t_{k+1}-\varsigma)^{\omega-1}d\varsigma
\end{aligned}
$$

$$C_{k+1} = C_0 + \frac{1-\omega}{AB(\omega)} t_k^{1-\varpi} C_1(t_k, S(t_k), C(t_k), I(t_k), R(t_k), P(t_k)) + \hbar \sum_{i=2}^{k} C_1[t_{i-2}, S^{i-2}, C^{i-2}, I^{i-2}, R^{i-2}, P^{i-2}] t_{i-2}^{1-\varpi}$$
$$\times \int_{t_i}^{t_{i+1}} (t_{k+1} - \varsigma)^{\omega-1} d\varsigma + \hbar \sum_{i=2}^{k} \frac{1}{\triangle t} \Big\{ t_{i-1}^{1-\varpi} C_1(t_{i-1}, S^{i-1}, C^{i-1}, I^{i-1}, R^{i-1}, P^{i-1}) - t_{i-2}^{1-\varpi} C_1[t_{i-2}, S^{i-2}, C^{i-2},$$
$$I^{i-2}, R^{i-2}, P^{i-2}] \Big\} \times \int_{t_i}^{t_{i+1}} (\varsigma - t_{i-2})(t_{k+1} - \varsigma)^{\omega-1} d\varsigma + \hbar \sum_{i=2}^{k} \frac{1}{2\triangle t^2} \Big\{ t_i^{1-\varpi} C_1[t_i, S^i, C^i, I^i, R^i, P^i] -$$
$$2t_{i-1}^{1-\varpi} C_1(t_{i-1}, S^{i-1}, C^{i-1}, I^{i-1}, R^{i-1}, P^{i-1}) + t_{i-2}^{1-\varpi} C_1[t_{i-2}, S^{i-2}, C^{i-2}, I^{i-2}, R^{i-2}, P^{i-2}] \Big\}$$
$$\times \int_{t_i}^{t_{i+1}} (\varsigma - t_{i-2})(\varsigma - t_{i-1})(t_{k+1} - \varsigma)^{\omega-1} d\varsigma$$

$$I_{k+1} = I_0 + \frac{1-\omega}{AB(\omega)} t_k^{1-\varpi} I_1(t_k, S(t_k), C(t_k), I(t_k), R(t_k), P(t_k)) + \hbar \sum_{i=2}^{k} I_1[t_{i-2}, S^{i-2}, C^{i-2}, I^{i-2}, R^{i-2}, P^{i-2}] t_{i-2}^{1-\varpi}$$
$$\times \int_{t_i}^{t_{i+1}} (t_{k+1} - \varsigma)^{\omega-1} d\varsigma + \hbar \sum_{i=2}^{k} \frac{1}{\triangle t} \Big\{ t_{i-1}^{1-\varpi} I_1(t_{i-1}, S^{i-1}, C^{i-1}, I^{i-1}, R^{i-1}, P^{i-1}) - t_{i-2}^{1-\varpi} I_1[t_{i-2}, S^{i-2}, C^{i-2},$$
$$I^{i-2}, R^{i-2}, P^{i-2}] \Big\} \times \int_{t_i}^{t_{i+1}} (\varsigma - t_{i-2})(t_{k+1} - \varsigma)^{\omega-1} d\varsigma + \hbar \sum_{i=2}^{k} \frac{1}{2\triangle t^2} \Big\{ t_i^{1-\varpi} I_1[t_i, S^i, C^i, I^i, R^i, P^i] -$$
$$2t_{i-1}^{1-\varpi} I_1(t_{i-1}, S^{i-1}, C^{i-1}, I^{i-1}, R^{i-1}, P^{i-1}) + t_{i-2}^{1-\varpi} I_1[t_{i-2}, S^{i-2}, C^{i-2}, I^{i-2}, R^{i-2}, P^{i-2}] \Big\}$$
$$\times \int_{t_i}^{t_{i+1}} (\varsigma - t_{i-2})(\varsigma - t_{i-1})(t_{k+1} - \varsigma)^{\omega-1} d\varsigma$$

$$R_{k+1} = R_0 + \frac{1-\omega}{AB(\omega)} t_k^{1-\varpi} R_1(t_k, S(t_k), C(t_k), I(t_k), R(t_k), P(t_k)) + \hbar \sum_{i=2}^{k} R_1[t_{i-2}, S^{i-2}, C^{i-2}, I^{i-2}, R^{i-2}, P^{i-2}] t_{i-2}^{1-\varpi}$$
$$\times \int_{t_i}^{t_{i+1}} (t_{k+1} - \varsigma)^{\omega-1} d\varsigma + \hbar \sum_{i=2}^{k} \frac{1}{\triangle t} \Big\{ t_{i-1}^{1-\varpi} R_1(t_{i-1}, S^{i-1}, C^{i-1}, I^{i-1}, R^{i-1}, P^{i-1}) - t_{i-2}^{1-\varpi} R_1[t_{i-2}, S^{i-2}, C^{i-2},$$
$$I^{i-2}, R^{i-2}, P^{i-2}] \Big\} \times \int_{t_i}^{t_{i+1}} (\varsigma - t_{i-2})(t_{k+1} - \varsigma)^{\omega-1} d\varsigma + \hbar \sum_{i=2}^{k} \frac{1}{2\triangle t^2} \Big\{ t_i^{1-\varpi} S_1[t_i, S^i, C^i, I^i, R^i, P^i] -$$
$$2t_{i-1}^{1-\varpi} R_1(t_{i-1}, S^{i-1}, C^{i-1}, I^{i-1}, R^{i-1}, P^{i-1}) + t_{i-2}^{1-\varpi} R_1[t_{i-2}, S^{i-2}, C^{i-2}, I^{i-2}, R^{i-2}, P^{i-2}] \Big\}$$
$$\times \int_{t_i}^{t_{i+1}} (\varsigma - t_{i-2})(\varsigma - t_{i-1})(t_{k+1} - \varsigma)^{\omega-1} d\varsigma$$

$$P_{k+1} = P_0 + \frac{1-\omega}{AB(\omega)} t_k^{1-\varpi} P_1(t_k, S(t_k), C(t_k), I(t_k), R(t_k), P(t_k)) + \hbar \sum_{i=2}^{k} P_1[t_{i-2}, S^{i-2}, C^{i-2}, I^{i-2}, R^{i-2}, P^{i-2}] t_{i-2}^{1-\varpi}$$
$$\times \int_{t_i}^{t_{i+1}} (t_{k+1} - \varsigma)^{\omega-1} d\varsigma + \hbar \sum_{i=2}^{k} \frac{1}{\triangle t} \Big\{ t_{i-1}^{1-\varpi} P_1(t_{i-1}, S^{i-1}, C^{i-1}, I^{i-1}, R^{i-1}, P^{i-1}) - t_{i-2}^{1-\varpi} P_1[t_{i-2}, S^{i-2}, C^{i-2},$$
$$I^{i-2}, R^{i-2}, P^{i-2}] \Big\} \times \int_{t_i}^{t_{i+1}} (\varsigma - t_{i-2})(t_{k+1} - \varsigma)^{\omega-1} d\varsigma + \hbar \sum_{i=2}^{k} \frac{1}{2\triangle t^2} \Big\{ t_i^{1-\varpi} S_1[t_i, S^i, C^i, I^i, R^i, P^i] -$$
$$2t_{i-1}^{1-\varpi} P_1(t_{i-1}, S^{i-1}, C^{i-1}, I^{i-1}, R^{i-1}, P^{i-1}) + t_{i-2}^{1-\varpi} P_1[t_{i-2}, S^{i-2}, C^{i-2}, I^{i-2}, R^{i-2}, P^{i-2}] \Big\}$$
$$\times \int_{t_i}^{t_{i+1}} (\varsigma - t_{i-2})(\varsigma - t_{i-1})(t_{k+1} - \varsigma)^{\omega-1} d\varsigma$$

We have

$$\int_{t_i}^{t_{i+1}}(t_{k+1}-\varsigma)^{\omega-1}d\varsigma=\frac{(\triangle t)^{\omega}}{\omega}\left[(k-i+1)^{\omega}-(k-i)^{\omega}\right]$$

$$\int_{t_i}^{t_{i+1}}(\varsigma-t_{i-2})(t_{k+1}-\varsigma)^{\omega-1}d\varsigma=\frac{(\triangle t)^{\omega+1}}{\omega(\omega+1)}\left[(k-i+1)^{\omega}(k-i+3+2\omega)-(k-i)^{\omega}(k-i+3+3\omega)\right]$$

$$\begin{aligned}\int_{t_i}^{t_{i+1}}(\varsigma-t_{i-2})(\varsigma-t_{i-1})(t_{k+1}-\varsigma)^{\omega-1}d\varsigma=\frac{(\triangle t)^{\omega+2}}{\omega(\omega+1)(\omega+2)}\Bigg[&(k-i+1)^{\omega}\\&\times\Big\{2(k-i)^2+(3\omega+10)(k-i)+2\omega^2+9\omega+12\Big\}\\&-(k-i)^{\omega}\Big\{2(k-i)^2+(5\omega+10)(k-i)+6\omega^2+18\omega+12\Big\}\Bigg]\end{aligned}$$

Therefore, we obtain

$$\begin{aligned}S_{k+1}=&\,S_0+\frac{1-\omega}{AB(\omega)}t_k^{1-\varpi}S_1(t_k,S(t_k),C(t_k),I(t_k),R(t_k),P(t_k))\\&+\hbar\sum_{i=2}^{k}S_1[t_{i-2},S^{i-2},C^{i-2},I^{i-2},R^{i-2},P^{i-2}]t_{i-2}^{1-\varpi}\times Q_1\\&+\hbar\sum_{i=2}^{k}\frac{1}{\triangle t}\Big\{t_{i-1}^{1-\varpi}S_1(t_{i-1},S^{i-1},C^{i-1},I^{i-1},R^{i-1},P^{i-1})-t_{i-2}^{1-\varpi}S_1[t_{i-2},S^{i-2},C^{i-2},I^{i-2},R^{i-2},P^{i-2}]\Big\}\times Q_2\\&+\hbar\sum_{i=2}^{k}\frac{1}{2\triangle t^2}\Big\{t_i^{1-\varpi}S_1[t_i,S^i,C^i,I^i,R^i,P^i]-2t_{i-1}^{1-\varpi}S_1(t_{i-1},S^{i-1},C^{i-1},I^{i-1},R^{i-1},P^{i-1})\\&+t_{i-2}^{1-\varpi}S_1[t_{i-2},S^{i-2},C^{i-2},I^{i-2},R^{i-2},P^{i-2}]\Big\}\times Q_3,\end{aligned}$$

where

$$\begin{aligned}Q_1&=\frac{(\triangle t)^{\omega}}{\omega}\left[(k-i+1)^{\omega}-(k-i)^{\omega}\right]\\Q_2&=\frac{(\triangle t)^{\omega+1}}{\omega(\omega+1)}\left[(k-i+1)^{\omega}(k-i+3+2\omega)-(k-i)^{\omega}(k-i+3+3\omega)\right]\\Q_3&=\frac{(\triangle t)^{\omega+2}}{\omega(\omega+1)(\omega+2)}\Bigg[(k-i+1)^{\omega}\Big\{2(k-i)^2+(3\omega+10)(k-i)+2\omega^2+\\&\quad 9\omega+12\Big\}-(k-i)^{\omega}\Big\{2(k-i)^2+(5\omega+10)(k-i)+6\omega^2+18\omega+12\Big\}\end{aligned}$$

$$\begin{aligned}C_{k+1}=&\,C_0+\frac{1-\omega}{AB(\omega)}t_k^{1-\varpi}C_1(t_k,S(t_k),C(t_k),I(t_k),R(t_k),P(t_k))\\&+\hbar\sum_{i=2}^{k}C_1[t_{i-2},S^{i-2},C^{i-2},I^{i-2},R^{i-2},P^{i-2}]t_{i-2}^{1-\varpi}\times Q_1\\&+\hbar\sum_{i=2}^{k}\frac{1}{\triangle t}\Big\{t_{i-1}^{1-\varpi}C_1(t_{i-1},S^{i-1},C^{i-1},I^{i-1},R^{i-1},P^{i-1})-t_{i-2}^{1-\varpi}C_1[t_{i-2},S^{i-2},C^{i-2},I^{i-2},R^{i-2},P^{i-2}]\Big\}\times Q_2\\&+\hbar\sum_{i=2}^{k}\frac{1}{2\triangle t^2}\Big\{t_i^{1-\varpi}C_1[t_i,S^i,C^i,I^i,R^i,P^i]-2t_{i-1}^{1-\varpi}C_1(t_{i-1},S^{i-1},C^{i-1},I^{i-1},R^{i-1},P^{i-1})\\&+t_{i-2}^{1-\varpi}C_1[t_{i-2},S^{i-2},C^{i-2},I^{i-2},R^{i-2},P^{i-2}]\Big\}\times Q_3,\end{aligned}$$

$$
\begin{aligned}
I_{k+1} &= I_0 + \frac{1-\omega}{AB(\omega)} t_k^{1-\varpi} I_1(t_k, S(t_k), C(t_k), I(t_k), R(t_k), P(t_k)) \\
&+ \hbar \sum_{i=2}^{k} I_1[t_{i-2}, S^{i-2}, C^{i-2}, I^{i-2}, R^{i-2}, P^{i-2}] t_{i-2}^{1-\varpi} \times Q_1 \\
&+ \hbar \sum_{i=2}^{k} \frac{1}{\triangle t} \left\{ t_{i-1}^{1-\varpi} I_1(t_{i-1}, S^{i-1}, C^{i-1}, I^{i-1}, R^{i-1}, P^{i-1}) - t_{i-2}^{1-\varpi} I_1[t_{i-2}, S^{i-2}, C^{i-2}, I^{i-2}, R^{i-2}, P^{i-2}] \right\} \times Q_2 \\
&+ \hbar \sum_{i=2}^{k} \frac{1}{2\triangle t^2} \left\{ t_i^{1-\varpi} I_1[t_i, S^i, C^i, I^i, R^i, P^i] - 2t_{i-1}^{1-\varpi} I_1(t_{i-1}, S^{i-1}, C^{i-1}, I^{i-1}, R^{i-1}, P^{i-1}) \right. \\
&\left. + t_{i-2}^{1-\varpi} I_1[t_{i-2}, S^{i-2}, C^{i-2}, I^{i-2}, R^{i-2}, P^{i-2}] \right\} \times Q_3,
\end{aligned}
$$

$$
\begin{aligned}
R_{k+1} &= R_0 + \frac{1-\omega}{AB(\omega)} t_k^{1-\varpi} R_1(t_k, S(t_k), C(t_k), I(t_k), R(t_k), P(t_k)) \\
&+ \hbar \sum_{i=2}^{k} R_1[t_{i-2}, S^{i-2}, C^{i-2}, I^{i-2}, R^{i-2}, P^{i-2}] t_{i-2}^{1-\varpi} \times Q_1 \\
&+ \hbar \sum_{i=2}^{k} \frac{1}{\triangle t} \left\{ t_{i-1}^{1-\varpi} R_1(t_{i-1}, S^{i-1}, C^{i-1}, I^{i-1}, R^{i-1}, P^{i-1}) - t_{i-2}^{1-\varpi} R_1[t_{i-2}, S^{i-2}, C^{i-2}, I^{i-2}, R^{i-2}, P^{i-2}] \right\} \times Q_2 \\
&+ \hbar \sum_{i=2}^{k} \frac{1}{2\triangle t^2} \left\{ t_i^{1-\varpi} R_1[t_i, S^i, C^i, I^i, R^i, P^i] - 2t_{i-1}^{1-\varpi} R_1(t_{i-1}, S^{i-1}, C^{i-1}, I^{i-1}, R^{i-1}, P^{i-1}) \right. \\
&\left. + t_{i-2}^{1-\varpi} R_1[t_{i-2}, S^{i-2}, C^{i-2}, I^{i-2}, R^{i-2}, P^{i-2}] \right\} \times Q_3,
\end{aligned}
$$

$$
\begin{aligned}
P_{k+1} &= P_0 + \frac{1-\omega}{AB(\omega)} t_k^{1-\varpi} P_1(t_k, S(t_k), C(t_k), I(t_k), R(t_k), P(t_k)) \\
&+ \hbar \sum_{i=2}^{k} P_1[t_{i-2}, S^{i-2}, C^{i-2}, I^{i-2}, R^{i-2}, P^{i-2}] t_{i-2}^{1-\varpi} \times Q_1 \\
&+ \hbar \sum_{i=2}^{k} \frac{1}{\triangle t} \left\{ t_{i-1}^{1-\varpi} P_1(t_{i-1}, S^{i-1}, C^{i-1}, I^{i-1}, R^{i-1}, P^{i-1}) - t_{i-2}^{1-\varpi} P_1[t_{i-2}, S^{i-2}, C^{i-2}, I^{i-2}, R^{i-2}, P^{i-2}] \right\} \times Q_2 \\
&+ \hbar \sum_{i=2}^{k} \frac{1}{2\triangle t^2} \left\{ t_i^{1-\varpi} P_1[t_i, S^i, C^i, I^i, R^i, P^i] - 2t_{i-1}^{1-\varpi} P_1(t_{i-1}, S^{i-1}, C^{i-1}, I^{i-1}, R^{i-1}, P^{i-1}) \right. \\
&\left. + t_{i-2}^{1-\varpi} P_1[t_{i-2}, S^{i-2}, C^{i-2}, I^{i-2}, R^{i-2}, P^{i-2}] \right\} \times Q_3,
\end{aligned}
$$

### *5.10 Simulation Explanation*

The following examples demonstrate the efficacy of the obtained theoretical consequences. A mathematical analysis of maize foliar disease is presented, and by using non-integer parametric parameters, compelling results are obtained. By reducing the fractional values and the dimension, the answer for $S, C, I, R$, and $P$ in Figure 2-6 approaches the desired value. The numerical simulation for the fractional order Maize foliar disease model is found using MATLAB code. The system's initial values are $S(0) = 1, C(0) = 0.8, I(0) = 0.750, R(0) = 0.50$, and $P(0) = 0.350$ for each of the sub-compartments. We show the graphical representation of the maize foliar disease model using the suggested numerical method in Figures 2-6, and we compare the integer order result with the fractal-fractional order result. The dynamics of susceptible $S$, recovered $R$ and $P$ maize foliar of pathogens are shown in Figures 2, 5 and 6, respectively. In these scenarios, all of the compartments had a sloped upward inclination, and after some time, as the recovered situation increased, the compartments approached a stable state. The dynamics of control $C$ and infected $I$ are shown in Figures 3 and 4, respectively. In these scenarios, all of the compartments rigidly sloped downward, and after a while, they

approached a steady position because to a rise in recovered. Figures 2a-6a and 2b-6b, respectively, show that while behaviors are comparable when using dimensions of 0.8 and 0.9 with small impacts, decreasing dimensions yields more acceptable results. Additionally, as shown in Figures 5a and 5b, respectively, recovered trees with and without medicine grow by decreasing the fractional values and dimension. It makes predictions on what this research will lead to in the future and how we will be able to lower the number of sick trees and infected vectors that spread throughout the environment. When compared to traditional derivatives, the FFM technique yields better results for all sub-compartments at fractional derivatives. It is also suggested that as fractional values and dimensions are reduced, the solutions for all compartments become more reliable and accurate.

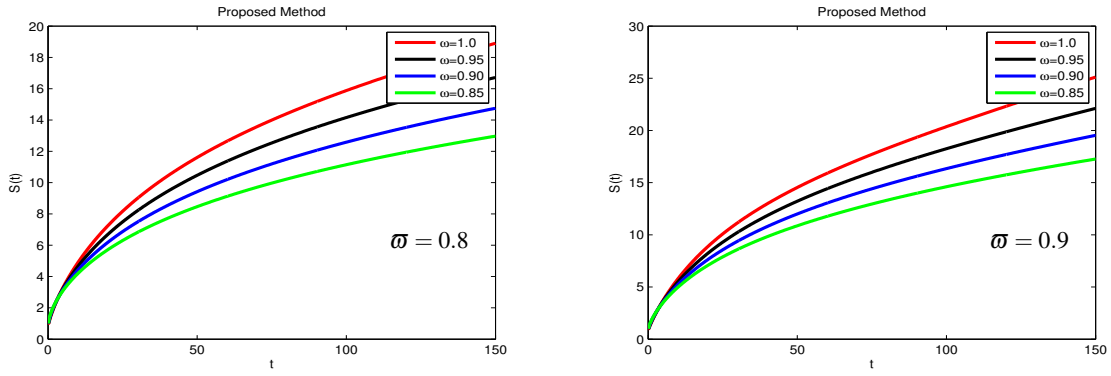


**Fig. 2:** Simulation of S(t) compartment of the system under different fractal dimension $\varpi$ and fractional order $\omega$.

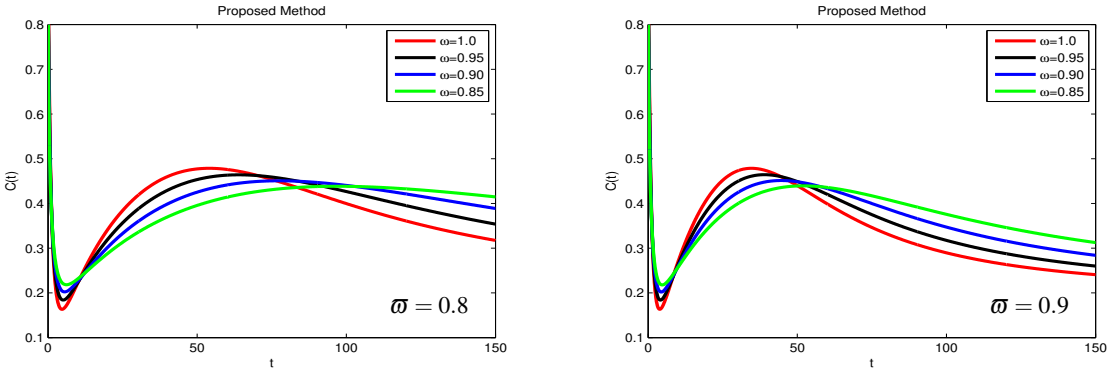


**Fig. 3:** Simulation of C(t) compartment of the system under different fractal dimension $\varpi$ and fractional order $\omega$.

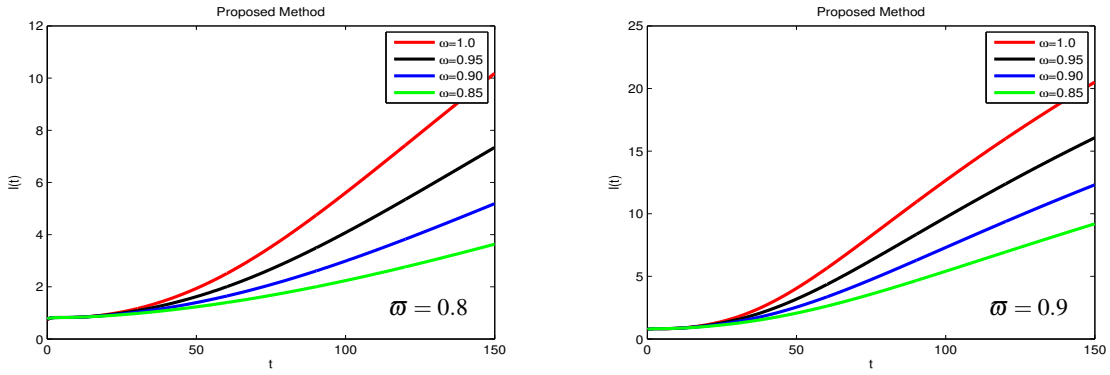


**Fig. 4:** Simulation of I(t) compartment of the system under different fractal dimension $\varpi$ and fractional order $\omega$.

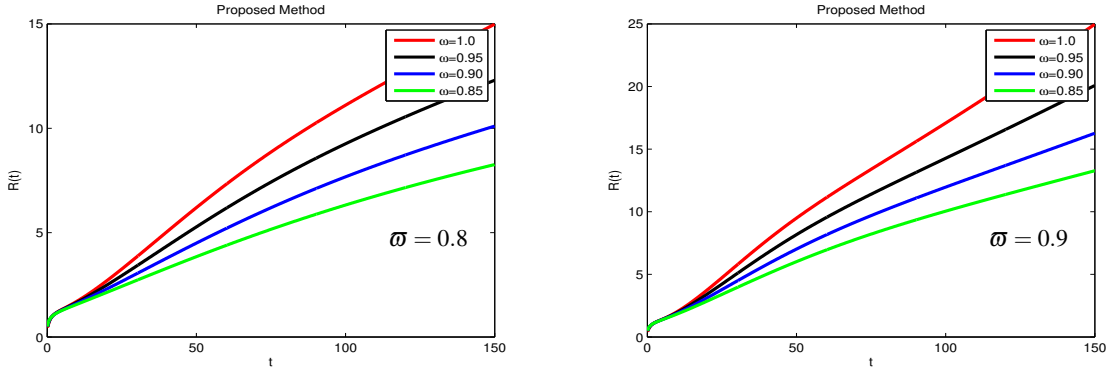


**Fig. 5:** Simulation of R(t) compartment of the system under different fractal dimension $\varpi$ and fractional order $\omega$.

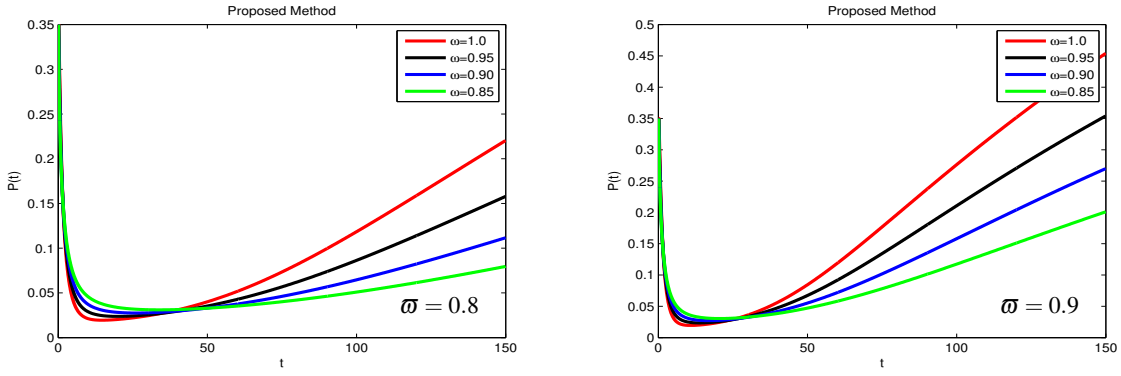


**Fig. 6:** Simulation of P(t) compartment of the system under different fractal dimension $\varpi$ and fractional order $\omega$.

## 6 Conclusions

Planning, controlling, and eradicating the negative effects of communicable illnesses from their early stages are the main goals of mathematical modeling. Because fractional order models have a different memory impact than classical models, they are helpful tools for assigning control actions wisely and optimizing resource consumption. Using the fractal-fractional operator to get dependable findings, the study generated a mathematical structural model for maize foliar disease that recovered without the need for medication. It recommends adding immune-system-strong compartments to stop the spread of disease. The study also looks at how the illness affects the population, with particular attention to the structure of vector-borne plant epidemics and the Beddington-DeAngelis functional response type infection rate. This research investigates a continuous dynamical system and verifies its stability as well as its ability to provide distinct answers for the fractional order maize foliar disease model. The disease is verified to exist, and its impact on global endeavors is evaluated. The research guarantees the validity and applicability of its conclusions by examining changes in infection rates following asymptomatic intervention. Plants with the disease show signs of rapid recovery when the fractal-fractional operator is used to monitor the disease's spread. The spread of the illness within the community is monitored through numerical simulations. In order to emphasize historical changes in epidemic models, this study ties together existing literature with unique fractional derivatives, a mixture of existing fractional operators. It also implies that authorities can make good use of several numerical techniques in addition to fractional epidemic models. When it comes to modeling some phenomena, fractional operators perform better than traditional derivatives and integrals. Unlike integer order derivatives, which only concentrate on one unique place, they take into account both previous data and current conditions, making them a better description of complicated nonlinear processes and high-order dynamics. Numerical results across a variety of fractional values demonstrate stable behavior of the two-step Lagrange polynomial approach in the equilibrium site for maize foliar disease. A potential approach to comprehending and forecasting the dynamics of infectious diseases is the use of fractional epidemic models. However, obstacles in research and real-world applications prevent their wider implementation. It can be challenging to obtain real-time data for parameter estimation and validation in environments with limited resources, especially during rapidly spreading epidemics. Another obstacle may be explaining the advantages to public health and policymakers. It is crucial to close the gap between mathematical intricacy and real-world application in order to overcome these obstacles. The models have proven to be accurate and reliable in a variety of epidemiological settings, underscoring their potential as useful tools for disease control initiatives. Future research can foresee patterns based on validated findings, which can aid in early identification and better comprehend the dynamics and behavior of maize foliar disease outbreaks. Future research could benefit from new understandings gained from this data. The mathematical model can be altered by examining various dynamic structures and using different derivatives. Real data for numerical simulations can assess model behavior for each class over time, validating the model for agreeing engineering and plant life improvement that play an important role for the economy of any country in terms of food and some other life materials.

## Acknowledgment

The authors extend their appreciation to Prince Sattam bin Abdulaziz University for funding this research work through the project number (2023/RV/04).

## Conflict of interest statement

Authors has no conflict of interest.

## References

[1] Lee, S., & Clinedinst, L. (2020). Mathematical biology: Expand, expose, and educate!. *Bulletin of Mathematical Biology*, 82(9), 120.

[2] Thornhill, J. P., Barkati, S., Walmsley, S., Rockstroh, J., Antinori, A., Harrison, L. B., ... & Orkin, C. M. (2022). Monkeypox virus infection in humans across 16 countries—April–June 2022. *New England Journal of Medicine*, 387(8), 679-691.

[3] Srivastava, H. M., Shanker Dubey, R., & Jain, M. (2019). A study of the fractional-order mathematical model of diabetes and its resulting complications. *Mathematical Methods in the Applied Sciences*, 42(13), 4570-4583.

[4] Bilgil, H., Yousef, A., Erciyes, A., Erdinç, Ü., & Öztürk, Z. (2023). A fractional-order mathematical model based on vaccinated and infected compartments of SARS-CoV-2 with a real case study during the last stages of the epidemiological event. *Journal of computational and applied mathematics*, 425, 115015.

[5] Zhang, Z., Zhang, W., Nisar, K. S., Gul, N., Zeb, A., & Vijayakumar, V. (2023). Dynamical aspects of a tuberculosis transmission model incorporating vaccination and time delay. *Alexandria Engineering Journal*, 66, 287-300.
[6] Ahmad, A., Ahmad, I., Ali, R., & Ibrahim, M. (2023). On analysis of fractional order HIV infection model with the adaptive immune response under Caputo operator. *Journal of Applied Mathematics and Computing*, 69(2), 1845-1863.
[7] Algehyne, E. A., & Ibrahim, M. (2021). Fractal-fractional order mathematical vaccine model of COVID-19 under non-singular kernel. *Chaos, Solitons & Fractals*, 150, 111150.
[8] Alnahdi, A. S., Jeelani, M. B., Wahash, H. A., & Abdulwasaa, M. A. (2023). A detailed mathematical analysis of the vaccination model for COVID-19. *CMES-Comput. Model. Eng. Sci*, 135, 1315-1343.
[9] Brauer, F. (2017). Mathematical epidemiology: Past, present, and future. *Infectious Disease Modelling*, 2(2), 113-127.
[10] Khan, M. A., Ahmad, M., Ullah, S., Farooq, M., & Gul, T. (2019). Modeling the transmission dynamics of tuberculosis in Khyber Pakhtunkhwa Pakistan. *Advances in Mechanical Engineering*, 11(6), 1687814019854835.
[11] Takasu, F. (2009). Individual-based modeling of the spread of pine wilt disease: vector beetle dispersal and the Allee effect. *Population Ecology*, 51, 399-409.
[12] Mota, M. M., Braasch, H., Bravo, M. A., Penas, A. C., Burgermeister, W., Metge, K., & Sousa, E. (1999). First report of Bursaphelenchus xylophilus in Portugal and in Europe. *Nematology*, 1(7), 727-734.
[13] Zhao, B. G., Futai, K., Sutherland, J. R., & Takeuchi, Y. (Eds.). (2008). Pine wilt disease (Vol. 17, p. 459). Tokyo, Japan:: *Springer*.
[14] Leonberger, K., Jackson, K., Smith, R., & Ward Gauthier, N. (2016). Plant diseases [2016].
[15] Lee, K. S., & Kim, D. (2013). Global dynamics of a pine wilt disease transmission model with nonlinear incidence rates. *Applied Mathematical Modelling*, 37(6), 4561-4569.
[16] Shi, X., & Song, G. (2013). Analysis of the mathematical model for the spread of pine wilt disease. *Journal of Applied Mathematics*, 2013.
[17] Lee, K. S., & Lashari, A. A. (2014). Global stability of a host-vector model for pine wilt disease with nonlinear incidence rate. *In Abstract and Applied Analysis* (Vol. 2014). Hindawi.
[18] Lia, Y., Haq, F., Shah, K., Shahzad, M., & Rahman, G. U. (2017). Numerical analysis of fractional order Pine wilt disease model with bilinear incident rate. *Journal of Mathematics and Computer Science*, 17, 420-428.
[19] Yoshimura, A., Kawasaki, K., Takasu, F., Togashi, K., Futai, K., & Shigesada, N. (1999). Modeling the spread of pine wilt disease caused by nematodes with pine sawyers as vector. *Ecology*, 80(5), 1691-1702.
[20] Kiyohara, T., & Bolla, R. I. (1990). Pathogenic variability among populations of the pinewood nematode, Bursaphelenchus xylophilus. *Forest Science*, 36(4), 1061-1076.
[21] Togashi, K., & Shigesada, N. (2006). Spread of the pinewood nematode vectored by the Japanese pine sawyer: modeling and analytical approaches. *Population Ecology*, 48, 271-283.
[22] Ryss, A. Y., Kulinich, O. A., & Sutherland, J. R. (2011). Pine wilt disease: a short review of worldwide research. *Forestry Studies in China*, 13, 132-138.
[23] Jones, J. D., & Dangl, J. L. (2006). The plant immune system. *nature*, 444(7117), 323-329. [PubMed] [CrossRef] [Google Scholar]
[24] Almeida, R. P. (2008). Ecology of emerging vector-borne plant diseases. *Vector-borne diseases: understanding the environmental, human health, and ecological connections*, 70-77. [PubMed] [Google Scholar]
[25] Jeger, M. J., Madden, L. V., & Van Den Bosch, F. (2018). Plant virus epidemiology: Applications and prospects for mathematical modeling and analysis to improve understanding and disease control. *Plant disease*, 102(5), 837-854. [PubMed] [CrossRef] [Google Scholar]
[26] Luo, Y., Gao, S., Xie, D., & Dai, Y. (2015). A discrete plant disease model with roguing and replanting. *Advances in Difference Equations*, 2015, 1-18.
[27] Sisterson, M. S., & Stenger, D. C. (2013). Roguing with replacement in perennial crops: conditions for successful disease management. *Phytopathology*, 103(2), 117-128.
[28] Jeger, M. J., Holt, J., Van Den Bosch, F., & Madden, L. V. (2004). Epidemiology of insect-transmitted plant viruses: modelling disease dynamics and control interventions. *Physiological Entomology*, 29(3), 291-304.
[29] Venturino, E., Roy, P. K., Al Basir, F., & Datta, A. (2016). A model for the control of the mosaic virus disease in Jatropha curcas plantations. *Energy, Ecology and Environment*, 1, 360-369.
[30] Buonomo, B., & Cerasuolo, M. (2014). Stability and bifurcation in plant–pathogens interactions. *Applied Mathematics and Computation*, 232, 858-871.
[31] Anggriani, N., Istifadah, N., Hanifah, M., & Supriatna, A. K. (2016). A mathematical model of protectant and curative fungicide application and its stability analysis. *In IOP conference series: earth and environmental science* (Vol. 31, No. 1, p. 012014). IOP Publishing.
[32] Anggriani, N., Ndii, M. Z., Arumi, D., Istifadah, N., & Supriatna, A. K. (2018, November). Mathematical model for plant disease dynamics with curative and preventive treatments. *In AIP Conference Proceedings* (Vol. 2043, No. 1). AIP Publishing.
[33] Jackson, M., & Chen-Charpentier, B. M. (2017). Modeling plant virus propagation with delays. *Journal of Computational and Applied Mathematics*, 309, 611-621.
[34] Jackson, M., & Chen-Charpentier, B. M. (2018). A model of biological control of plant virus propagation with delays. *Journal of Computational and Applied Mathematics*, 330, 855-865.

[35] Meng, X., & Li, Z. (2010). The dynamics of plant disease models with continuous and impulsive cultural control strategies. *Journal of Theoretical Biology*, 266(1), 29-40.
[36] Zhang, T., Meng, X., Song, Y., & Li, Z. (Article ID 428453, Volume 2012, January). Dynamical analysis of delayed plant disease models with continuous or impulsive cultural control strategies. Abstract and Applied Analysis ,
[37] Shi, R., Zhao, H., & Tang, S. (2014). Global dynamic analysis of a vector-borne plant disease model. *Advances in Difference Equations*, 2014, 1-16. [CrossRef] [Google Scholar]
[38] Kumar, P., Baleanu, D., Erturk, V. S., Inc, M., & Govindaraj, V. (2022). A delayed plant disease model with Caputo fractional derivatives. *Advances in Continuous and Discrete Models*, 2022(1), 11.
[39] Sardar, T., Rana, S., Bhattacharya, S., Al-Khaled, K., & Chattopadhyay, J. (2015). A generic model for a single strain mosquito-transmitted disease with memory on the host and the vector. *Mathematical biosciences*, 263, 18-36.
[40] Achar, S. J., & K, G. N. (2024). Dynamics of fractional plant virus propagation model with influence of seasonality and intraspecific competition. *Mathematical Methods in the Applied Sciences*.
[41] Nisar, K. S., Logeswari, K., Vijayaraj, V., Baskonus, H. M., & Ravichandran, C. (2022). Fractional order modeling the gemini virus in capsicum annuum with optimal control. *Fractal and Fractional*, 6(2), 61.
[42] Liu, S., Huang, M., & Wang, J. (2020). Bifurcation control of a delayed fractional mosaic disease model for jatropha curcas with farming awareness. *Complexity*, 2020.
[43] Tilahun, G. T., Wolle, G. A., & Tofik, M. (2021). Eco-epidemiological model and analysis of potato leaf roll virus using fractional differential equation. *Arab Journal of Basic and Applied Sciences*, 28(1), 41-50.
[44] Liu, Y., Zeng, C., Guo, J., & Liao, Z. (2022). Global dynamics of a new Huanglongbing transmission model with quarantine measures. *Applied Mathematics*, 13(1), 1-18.
[45] Nazarov, P. A., Baleev, D. N., Ivanova, M. I., Sokolova, L. M., & Karakozova, M. V. (2020). Infectious plant diseases: Etiology, current status, problems and prospects in plant protection. *Acta naturae*, 12(3), 46.
[46] Nakasuji, F., Miyai, S., Kawamoto, H., & Kiritani, K. (1985). Mathematical epidemiology of rice dwarf virus transmitted by green rice leafhoppers: A differential equation model. *Journal of applied ecology*, 839-847.
[47] Degefa, D. S., Makinde, O. D., & Temesgen, D. T. (2022). Modeling potato virus Y disease dynamics in a mixed-cropping system. *International Journal of Modelling and Simulation*, 42(3), 370-387.
[48] Li, W., Huang, L., & Wang, J. (2020). Global dynamics of Filippov-type plant disease models with an interaction ratio threshold. *Mathematical Methods in the Applied Sciences*, 43(11), 6995-7008.
[49] Vellappandi, M., Kumar, P., Govindaraj, V., & Albalawi, W. (2022). An optimal control problem for mosaic disease via Caputo fractional derivative. *Alexandria Engineering Journal*, 61(10), 8027-8037.
[50] Kirtphaiboon, S., Humphries, U., Khan, A., & Yusuf, A. (2021). Model of rice blast disease under tropical climate conditions. *Chaos, Solitons & Fractals*, 143, 110530.
[51] Ali, H. M., & Ameen, I. G. (2023). Stability and optimal control analysis for studying the transmission dynamics of a fractional-order MSV epidemic model. *Journal of Computational and Applied Mathematics*, 434, 115352.
[52] Ameen, I. G., Baleanu, D., & Ali, H. M. (2022). Different strategies to confront maize streak disease based on fractional optimal control formulation. *Chaos, Solitons & Fractals*, 164, 112699.
[53] Wang, J., Feng, F., Guo, Z., Lv, H., & Wang, J. (2019). Threshold dynamics of a vector-borne epidemic model for Huanglongbing with impulsive control. *Applied Mathematics*, 10(4), 196-211.
[54] Ali, H. M., & Ameen, I. G. (2020). Save the pine forests of wilt disease using a fractional optimal control strategy. *Chaos, Solitons & Fractals*, 132, 109554.
[55] Mustafa, H. H., Samat, N. A., Mohamed, Z., & Kassim, F. A. (2021). Stage progression model for soil-borne plant disease in oil palm plantation. *Journal of Xi'an Shiyou University ISSN No*, 1673, 064X.
[56] Milici, C., Draganescu, G., & Machado, J. T. (2018). *Introduction to fractional differential equations* (Vol. 25). Springer.
[57] Hoan, L. V. C., Akinlar, M. A., Inc, M., Gómez-Aguilar, J. F., Chu, Y. M., & Almohsen, B. (2020). A new fractional-order compartmental disease model. *Alexandria Engineering Journal*, 59(5), 3187-3196.
[58] Evirgen, F. (2023). Transmission of Nipah virus dynamics under Caputo fractional derivative. *Journal of Computational and Applied Mathematics*, 418, 114654.
[59] Alyobi, S., & Jan, R. (2023). Qualitative and quantitative analysis of fractional dynamics of infectious diseases with control measures. *Fractal and Fractional*, 7(5), 400.
[60] Baker, R. E., Mahmud, A. S., Miller, I. F., Rajeev, M., Rasambainarivo, F., Rice, B. L., ... & Metcalf, C. J. E. (2022). Infectious disease in an era of global change. *Nature Reviews Microbiology*, 20(4), 193-205.
[61] Sweileh, W. M. (2022). Global research activity on mathematical modeling of transmission and control of 23 selected infectious disease outbreak. *Globalization and Health*, 18(1), 4.
[62] Khan, M. A., & Atangana, A. (2022). Mathematical modeling and analysis of COVID-19: A study of new variant Omicron. *Physica A: Statistical Mechanics and its Applications*, 599, 127452.
[63] Thirthar, A. A., Abboubakar, H., Khan, A., & Abdeljawad, T. (2023). Mathematical modeling of the COVID-19 epidemic with fear impact. *AIMS Math*, 8(3), 6447-6465.
[64] Zhang, Q., Liu, X., Li, Q., Liu, Y., He, H., Wang, K., & Yan, Z. (2023). Quantitative model for assessment of lower-extremity perfusion in patients with diabetes. *Medical Physics*, 50(5), 3019-3026.
[65] Andrawus, J., Abdulrahman, S., Singh, R. V. K., & Manga, S. S. (2022). Optimal Control of Mathematical Modelling for Ebola Virus Population Dynamics in the Presence of Vaccination. *Dutse Journal of Pure and Applied Sciences*, 8, 126-137.

[66] Kotola, B. S., & Mekonnen, T. T. (2022). Mathematical model analysis and numerical simulation for codynamics of meningitis and pneumonia infection with intervention. *Scientific Reports*, 12(1), 2639.
[67] Bolarin, G. (2014). On the dynamical analysis of a new model for measles infection. *International Journal of Mathematics Trends and Technology*, 7(2), 144-155.
[68] Viriyapong, R., & Ridbamroong, W. (2020). Global stability analysis and optimal control of measles model with vaccination and treatment. *Journal of Applied Mathematics and Computing*, 62, 207-237.
[69] Sowole, S. O., Ibrahim, A., Sangare, D., & Lukman, A. O. (2020). Mathematical model for measles disease with control on the susceptible and exposed compartments. *Open Journal of Mathematical Analysis*, 4(1), 60-75.
[70] Liu, P., Ikram, R., Khan, A., & Din, A. (2023). The measles epidemic model assessment under real statistics: an application of stochastic optimal control theory. *Computer Methods in Biomechanics and Biomedical Engineering*, 26(2), 138-159.
[71] Peter, O. J., Panigoro, H. S., Ibrahim, M. A., Otunuga, O. M., Ayoola, T. A., & Oladapo, A. O. (2023). Analysis and dynamics of measles with control strategies: A mathematical modeling approach. *International Journal of Dynamics and Control*, 11(5), 2538-2552.
[72] Wang, Y., Cao, J., Li, X., & Alsaedi, A. (2018). Edge-based epidemic dynamics with multiple routes of transmission on random networks. *Nonlinear Dynamics*, 91, 403-420.
[73] Ahmad, A., Farman, M., Ghafar, A., Inc, M., Ahmad, M. O., & Sene, N. (2022). Analysis and simulation of fractional order smoking epidemic model. *Computational and Mathematical Methods in Medicine*, 2022.
[74] Katugampola, U. N. (2011). A new approach to generalized fractional derivatives. *arXiv preprint arXiv*:1106.0965.
[75] Podlubny, I., Magin, R. L., & Trymorush, I. (2017). Niels Henrik Abel and the birth of fractional calculus. *Fractional Calculus and Applied Analysis*, 20(5), 1068-1075.
[76] De Oliveira, E. C., & Tenreiro Machado, J. A. (2014). A review of definitions for fractional derivatives and integral. *Mathematical Problems in Engineering*, 2014.
[77] Berhe, H. W., Makinde, O. D., & Theuri, D. M. (2019). Modelling the dynamics of direct and pathogens-induced dysentery diarrhoea epidemic with controls. *Journal of biological dynamics*, 13(1), 192-217.
[78] Caputo, M.,& Fabrizio, M. (2015). A new definition of fractional derivative without singular kernel. *Progress in Fractional Differentiation & Applications*, 1(2), 73-85.
[79] Atangana, A., & Baleanu, D. (2016, Vol 20, Issue 2, Pages: 763-769). New fractional derivatives with nonlocal and non-singular kernel: theory and application to heat transfer model. Thermal Science.
[80] Atangana, A. (2017). Fractal-fractional differentiation and integration: connecting fractal calculus and fractional calculus to predict complex system. *Chaos, Solitons & Fractals*, 102, 396-406.
[81] Li, Z., Liu, Z., & Khan, M. A. (2020). Fractional investigation of bank data with fractal-fractional Caputo derivative. *Chaos, Solitons & Fractals*, 131, 109528.
[82] Gao, W., Veeresha, P., Prakasha, D. G., Baskonus, H. M., & Yel, G. (2020). New approach for the model describing the deathly disease in pregnant women using Mittag-Leffler function. *Chaos, Solitons & Fractals*, 134, 109696.
[83] Zeb, A., Atangana, A., Khan, Z. A., & Djillali, S. (2022). A robust study of a piecewise fractional order COVID-19 mathematical model. *Alexandria Engineering Journal*, 61(7), 5649-5665.
[84] Farman, M., Malik, S. M., Akgül, A., & Salamat, N. (2023). Analysis and dynamical transmission of tuberculosis model with Treatment effect by using Fractional Operator. https://doi.org/10.21203/rs.3.rs-2438955/v1
[85] Anwarud, D. I. N., & Abidin, M. Z. (2022). Analysis of fractional-order vaccinated Hepatitis-B epidemic model with Mittag-Leffler kernels. *Mathematical Modelling and Numerical Simulation with Applications*, 2(2), 59-72.
[86] Zhang, L., Addai, E., Ackora-Prah, J., Arthur, Y. D., & Asamoah, J. K. K. (2022). Fractional-order Ebola-Malaria coinfection model with a focus on detection and treatment rate. *Computational and Mathematical Methods in Medicine*, 2022.
[87] Zafar, Z. U. A., Hussain, M. T., Inc, M., Baleanu, D., Almohsen, B., Oke, A. S., & Javeed, S. (2022). Fractional-order dynamics of human papillomavirus. *Results in Physics*, 34, 105281.
[88] Bonyah, E., Yavuz, M., Baleanu, D., & Kumar, S. (2022). A robust study on the listeriosis disease by adopting fractal-fractional operators. *Alexandria Engineering Journal*, 61(3), 2016-2028.
[89] Haq, I. U., Yavuz, M., Ali, N., & Akgül, A. (2022). A SARS-CoV-2 fractional-order mathematical model via the modified euler method. *Mathematical and Computational Applications*, 27(5), 82.
[90] Abdoon, M. A., Saadeh, R., Berir, M., & Guma, F. E. (2023). Analysis, modeling and simulation of a fractional-order influenza model. *Alexandria Engineering Journal*, 74, 231-240.
[91] Nisar, K. S., Farman, M., Hincal, E., & Shehzad, A. (2023). Modelling and analysis of bad impact of smoking in society with Constant Proportional-Caputo Fabrizio operator. *Chaos, Solitons & Fractals*, 172, 113549.
[92] Kumar, S., Chauhan, R. P., Osman, M. S., & Mohiuddine, S. A. (2023). A study on fractional HIV-AIDs transmission model with awareness effect. *Mathematical Methods in the Applied Sciences*, 46(7), 8334-8348.
[93] Baleanu, D., Shekari, P., Torkzadeh, L., Ranjbar, H., Jajarmi, A., & Nouri, K. (2023). Stability analysis and system properties of Nipah virus transmission: A fractional calculus case study. *Chaos, Solitons & Fractals*, 166, 112990.
[94] Azeem, M., Farman, M., Akgül, A., & De la Sen, M. (2023). Fractional order operator for symmetric analysis of cancer model on stem cells with chemotherapy. *Symmetry*, 15(2), 533.
[95] Abdullah, F. A., Liu, F., Burrage, P., Burrage, K., & Li, T. (2018). Novel analytical and numerical techniques for fractional temporal SEIR measles model. *Numerical Algorithms*, 79, 19-40.

[96] Almeida, R., & Qureshi, S. (2019). A fractional measles model having monotonic real statistical data for constant transmission rate of the disease. *Fractal and Fractional*, 3(4), 53.
[97] Nazir, G., Shah, K., Alrabaiah, H., Khalil, H., & Khan, R. A. (2020). Fractional dynamical analysis of measles spread model under vaccination corresponding to nonsingular fractional order derivative. *Advances in Difference Equations*, 2020(1), 171.
[98] Abdelaziz, M. A., Ismail, A. I., Abdullah, F. A., & Mohd, M. H. (2020). Codimension one and two bifurcations of a discrete-time fractional-order SEIR measles epidemic model with constant vaccination. *Chaos, Solitons & Fractals*, 140, 110104.
[99] Khan, A., Gomez-Aguilar, J. F., Abdeljawad, T., & Khan, H. (2020). Stability and numerical simulation of a fractional order plant-nectar-pollinator model. *Alexandria Engineering Journal*, 59(1), 49-59.
[100] ur Rahman, M., Arfan, M., & Baleanu, D. (2023). Piecewise fractional analysis of the migration effect in plant-pathogen-herbivore interactions. *Bulletin of Biomathematics*, 1(1), 1-23.
[101] Shah, K., Alqudah, M. A., Jarad, F., & Abdeljawad, T. (2020). Semi-analytical study of Pine Wilt Disease model with convex rate under Caputo–Febrizio fractional order derivative. *Chaos, Solitons & Fractals*, 135, 109754.
[102] Sawangtong, P., Logeswari, K., Ravichandran, C., Nisar, K. S., & Vijayaraj, V. (2023). Fractional order geminivirus impression in capsicum annuum model with Mittag-Leffler kernal. *Fractals*, 31(04), 2340049.
[103] Jan, A., Boulaaras, S., Abdullah, F. A., & Jan, R. (2023). Dynamical analysis, infections in plants, and preventive policies utilizing the theory of fractional calculus. *The European Physical Journal Special Topics*, 232(14), 2497-2512.
[104] Xu, C., Liu, Z., Li, P., Yan, J., & Yao, L. (2023). Bifurcation mechanism for fractional-order three-triangle multi-delayed neural networks. *Neural Processing Letters*, 55(5), 6125-6151.
[105] Farman, M., Nisar, K. S., Shehzad, A., Baleanu, D., Amjad, A., & Sultan, F. (2024). Computational analysis and chaos control of the fractional order syphilis disease model through modeling. *Ain Shams Engineering Journal*, 102743.
[106] Padder, A., Almutairi, L., Qureshi, S., Soomro, A., Afroz, A., Hincal, E., & Tassaddiq, A. (2023). Dynamical analysis of generalized tumor model with Caputo fractional-order derivative. *Fractal and Fractional*, 7(3), 258.
[107] Farman, M., Alfiniyah, C., & Saqib, M. (2024). Global Stability with Lyapunov Function and Dynamics of SEIR-Modified Lassa Fever Model in Sight Power Law Kernel. *Complexity*, 2024.
[108] Xu, C., Mu, D., Pan, Y., Aouiti, C., & Yao, L. (2023). Exploring bifurcation in a fractional-order predator-prey system with mixed delays. *J. Appl. Anal. Comput*, 13(3), 1119-1136.
[109] Jamil, S., Bariq, A., Farman, M., Nisar, K. S., Akgül, A., & Saleem, M. U. (2024). Qualitative analysis and chaotic behavior of respiratory syncytial virus infection in human with fractional operator. *Scientific Reports*, 14(1), 2175.
[110] Sabir, Z., Said, S. B., & Al-Mdallal, Q. (2023). A fractional order numerical study for the influenza disease mathematical model. *Alexandria Engineering Journal*, 65, 615-626.
[111] Naik, P. A., Farman, M., Zehra, A., Nisar, K. S., & Hincal, E. (2024). Analysis and modeling with fractal-fractional operator for an epidemic model with reference to COVID-19 modeling. *Partial Differential Equations in Applied Mathematics*, 100663.
[112] Alaje, A. I., & Olayiwola, M. O. (2023). A fractional-order mathematical model for examining the spatiotemporal spread of COVID-19 in the presence of vaccine distribution. *Healthcare Analytics*, 4, 100230.
[113] Prasad, R., Kumar, K., & Dohare, R. (2023). Caputo fractional order derivative model of Zika virus transmission dynamics. *J. Math. Comput. Sci*, 28(2), 145-157.
[114] Farman, M., Jamil, S., Nisar, K. S., & Akgül, A. (2024). Mathematical study of fractal-fractional leptospirosis disease in human and rodent populations dynamical transmission. *Ain Shams Engineering Journal*, 15(3), 102452.
[115] Mangal, S., Misra, O. P., & Dhar, J. (2023). Fractional-order deterministic epidemic model for the spread and control of HIV/AIDS with special reference to Mexico and India. *Mathematics and Computers in Simulation*, 210, 82-102.
[116] Batool, M., Farman, M., Ahmad, A., & Nisar, K. S. (2024). Mathematical study of polycystic ovarian syndrome disease including medication treatment mechanism for infertility in women. *AIMS Public Health*, 11(1), 19-35.
[117] Farman, M., Xu, C., Shehzad, A., & Akgül, A. (2024). Modelling and dynamics of measles via fractional differential operator of singular and non-singular kernels. *Mathematics and Computers in Simulation*.
[118] Farman, M., Shehzad, A., Akgül, A., Baleanu, D., Attia, N., & Hassan, A. M. (2023). Analysis of a fractional order Bovine Brucellosis disease model with discrete generalized Mittag–Leffler kernels. *Results in Physics*, 52, 106887.
[119] Ain, Q. T., Khan, A., Abdeljawad, T., Gómez-Aguilar, J. F., & Riaz, S. (2024). Dynamical study of varicella-zoster virus model in sense of Mittag-Leffler kernel. *International Journal of Biomathematics*, 17(03), 2350027.
[120] Huseynov, I. T., Ahmadova, A., & Mahmudov, N. I. (2020). Fractional Leibniz integral rules for Riemann-Liouville and Caputo fractional derivatives and their applications. *arXiv preprint arXiv*:2012.11360.
[121] Anderson, D. R., & Ulness, D. J. (2015). Newly defined conformable derivatives. *Adv. Dyn. Syst. Appl.*, 10(2), 109-137.
[122] Baleanu, D., Fernandez, A., & Akgül, A. (2020). On a fractional operator combining proportional and classical differintegrals. *Mathematics*, 8(3), 360.
[123] Ahmed, I., Kumam, P., Jarad, F., Borisut, P., & Jirakitpuwapat, W. (2020). On Hilfer generalized proportional fractional derivative. *Advances in Difference Equations*, 2020, 1-18.
[124] Kumar, P., Erturk, V. S., & Almusawa, H. (2021). Mathematical structure of mosaic disease using microbial biostimulants via Caputo and Atangana–Baleanu derivatives. *Results in Physics*, 24, 104186.
[125] Shah, K., Alqudah, M. A., Jarad, F., & Abdeljawad, T. (2020). Semi-analytical study of Pine Wilt Disease model with convex rate under Caputo–Febrizio fractional order derivative. *Chaos, Solitons & Fractals*, 135, 109754.

[126] Ackora-Prah, J., Seidu, B., Okyere, E., & Asamoah, J. K. (2023). Fractal-fractional caputo maize streak virus disease model. *Fractal and Fractional*, 7(2), 189.
[127] Shaw, P. K., Kumar, S., Momani, S., & Hadid, S. (2022). Dynamical analysis of fractional plant disease model with curative and preventive treatments. *Chaos, Solitons & Fractals*, 164, 112705.
[128] Kelderer, M., Manici, L. M., Caputo, F., & Thalheimer, M. (2012). Planting in the 'inter-row'to overcome replant disease in apple orchards: a study on the effectiveness of the practice based on microbial indicators. *Plant and Soil*, 357, 381-393.
[129] Manganiello, G., Nicastro, N., Caputo, M., Zaccardelli, M., Cardi, T., & Pane, C. (2021). Functional hyper spectral imaging by high-related vegetation indices to track the wide-spectrum Trichoderma biocontrol activity against soil-borne diseases of baby-leaf vegetables. *Frontiers in Plant Science*, 12, 630059.
[130] Manici, L. M., Kelderer, M., Franke-Whittle, I. H., Rühmer, T., Baab, G., Nicoletti, F., ... & Naef, A. (2013). Relationship between root-endophytic microbial communities and replant disease in specialized apple growing areas in Europe. *Applied soil ecology*, 72, 207-214.
[131] Farman, M., Sarwar, R., & Akgul, A. (2023). Modeling and analysis of sustainable approach for dynamics of infections in plant virus with fractal fractional operator. *Chaos, Solitons & Fractals*, 170, 113373.
[132] El-Sayed, A. M. A., Rida, S. Z., & Gaber, Y. A. (2020). Dynamical of curative and preventive treatments in a two-stage plant disease model of fractional order. *Chaos, Solitons & Fractals*, 137, 109879.
[133] Abdullah, T. Q., Huang, G., & Al-Sadi, W. (2022). A curative and preventive treatment fractional model for plant disease in Atangana–Baleanu derivative through Lagrange interpolation. *International Journal of Biomathematics*, 15(08), 2250052.
[134] Ali, H. M., Ameen, I. G., & Gaber, Y. A. (2024). The effect of curative and preventive optimal control measures on a fractional order plant disease model. *Mathematics and Computers in Simulation*.
[135] Kumar, S., Kumar, A., & Jleli, M. (2022). A numerical analysis for fractional model of the spread of pests in tea plants. *Numerical Methods for Partial Differential Equations*, 38(3), 540-565.
[136] Bonyah, E. (2022). A fractional dynamics of a potato disease model. *Commun. Math. Biol. Neurosci.*, 2022, Article-ID.
[137] Jeger, M. J., Van Den Bosch, F., Madden, L. V., & Holt, J. (1998). A model for analysing plant-virus transmission characteristics and epidemic development. *Mathematical Medicine and Biology: A Journal of the IMA*, 15(1), 1-18.
[138] Kahsay, B. N., & Makinde, O. D. (2023). Ecoepidemiological Model and Optimal Control Analysis of Tomato Yellow Leaf Curl Virus Disease in Tomato Plant. *Journal of Applied Mathematics*, 2023.
[139] Atangana, A. (2020). Modelling the spread of COVID-19 with new fractal-fractional operators: can the lockdown save mankind before vaccination?. *Chaos, Solitons & Fractals*, 136, 109860.
[140] Kumar, P., Baleanu, D., Erturk, V. S., Inc, M., & Govindaraj, V. (2022). A delayed plant disease model with Caputo fractional derivatives. *Advances in Continuous and Discrete Models*, 2022(1), 11.
[141] Vellappandi, M., Kumar, P., Govindaraj, V., & Albalawi, W. (2022). An optimal control problem for mosaic disease via Caputo fractional derivative. *Alexandria Engineering Journal*, 61(10), 8027-8037.
[142] Kumar, P., Erturk, V. S., Banerjee, R., Yavuz, M., & Govindaraj, V. (2021). Fractional modeling of plankton-oxygen dynamics under climate change by the application of a recent numerical algorithm. *Physica Scripta*, 96(12), 124044.
[143] Koca, I., Bulut, H., & Akçetin, E. (2022). A different approach for behavior of fractional plant virus model. *J. Nonlinear Sci. Appl*, 15, 186-202.
[144] Sajjad, A., Farman, M., Hasan, A., & Nisar, K. S. (2023). Transmission dynamics of fractional order yellow virus in red chili plants with the Caputo–Fabrizio operator. *Mathematics and Computers in Simulation*, 207, 347-368.
[145] Farman, M., Hasan, A., Sultan, M., Ahmad, A., Akgül, A., Chaudhry, F., ... & Weera, W. (2023). Yellow virus epidemiological analysis in red chili plants using Mittag-Leffler kernel. *Alexandria Engineering Journal*, 66, 811-825.
[146] Alqahtani, Z., & Hagag, A. E. (2023). A fractional numerical study on a plant disease model with replanting and preventive treatment. *Métodos numéricos para cálculo y diseño en ingeniería: Revista internacional*, 39(3), 1-21.
[147] Fantaye, A. K., & Birhanu, Z. K. (2023). Modeling and analysis for the transmission dynamics of cotton leaf curl virus using fractional order derivatives. *Heliyon*, 9(6).
[148] Collins, O. C., & Duffy, K. J. (2016). Optimal control of maize foliar diseases using the plants population dynamics. *Acta Agriculturae Scandinavica, Section B—Soil & Plant Science*, 66(1), 20-26.
[149] Kumar, A., Kumar, S., Alzaid, S. S., & Alkahtani, B. S. T. (2022). A novel mechanism to simulate fractional order maize foliar disease dynamical model. *Results in Physics*, 41, 105863.
[150] Putri, K. M. (2019, June). A maize foliar disease mathematical model with standard incidence rate. *In IOP Conference Series: Materials Science and Engineering* (Vol. 546, No. 5, p. 052085). IOP Publishing.